Relativistic Description of Heavy-Light Mesons

Timo Arvid Lähde

April 2000

Pro Gradu
M.Sc. Thesis

Department of Physics, POB 9, 00014
University of Helsinki / Helsingfors Universitet
Finland

Abstract

A method is presented for calculation of the spectra of mesons composed of a heavy quark (Q) and a light antiquark ($\bar{q}$). The method is based on the relativistic quasipotential reduction of the Bethe-Salpeter (BS) equation known as the Blankenbecler-Sugar (BSLT) equation. This method takes full account of the relativistic kinetic energy of the quark and antiquark. The BSLT equation is solved with the interaction between the quark and the antiquark modeled by screened one-gluon exchange (OGE) and a linear confining interaction. Explicit nonstatic expressions for the central and hyperfine components of the OGE interaction are given. The confining interaction is assumed to couple as a scalar invariant with a leading term that depends linearly on the quark separation. Methods for obtaining nonstatic expressions for the central and spin-orbit components of the local confining interaction are presented. The instanton induced interaction, which shares many features with the OGE interaction, is discussed. Predictions are given for the spectra of the D,D_s and B,B_s systems. Finally the quality of the model is tested by calculation of the spectrum of charmonium ($c\bar{c}$).

URN:NBN:fi-fe20001105

Contents

1 Introduction

The quark-antiquark bound state problem has been studied for several decades by means of perturbative Quantum Chromodynamics (QCD), numerical lattice simulations and other methods. Although much progress has been made, there still remain several aspects of $Q\bar{Q}$ and $Q\bar{q}$ systems, which are best addressed by phenomenological methods. These include the important phenomena of confinement and radiative decays. Completely phenomenological methods seem inadequate for these purposes, and indeed most modern calculations use some form of QCD motivated models, which are based on the one-gluon exchange (OGE) + linear confinement ansatz, which is clearly appropriate for heavy quarkonia. This has been widely used in the conventional nonrelativistic Schrödinger formalism, for example in [1, 17] and has generally been successful in accounting for most features of the heavy quarkonia. The Schrödinger formalism has also been used for very ambitious calculations, where the effective interaction has been extracted by means of lattice QCD and fitted to a Hamiltonian model [10].

In spite of this situation, there are still several areas where a phenomenological approach is necessary and even preferable. These include the confining interaction, since lattice studies are still severely limited by the processing power of computers available today. Consequently, the current knowledge of the long-range quark-antiquark interaction is limited [11]. Moreover, the question of the coupling structure of confinement is best addressed by phenomenological methods, in particular by studies of the M1 decay rates of heavy [17] and heavy-light [18] quarkonia. These spin-flip transitions obtain a significant contribution from the two-quark exchange current that appears if the confining interaction couples as a scalar in the spinor representation. This contribution turns out to be crucial for agreement with the observed decay rates [17]. In view of this, the confining interaction is assumed to couple as a scalar in this work. For the heavy-light systems, the situation is more complicated, not only because of the large relativistic and nonlocal effects that can be expected, but also because of the uncertain structure of the interaction between the heavy quark and the light antiquark. This being the case, the natural choice is to employ a quasipotential reduction of the Bethe-Salpeter equation in order to achieve a covariant treatment. In this work, the quasipotential reduction suggested by Blankenbecler, Sugar, Logunov and Tavkhelidze [2, 3] will be used. This approach is commonly referred to as the Blankenbecler-Sugar (BSLT) equation. This choice has the advantage of leading to a Lippmann-Schwinger type equation, while simultaneously taking full account of the relativistic kinetic energy operator. The modifications to the interaction are in comparison modest, and can be naturally accounted for if no approximation is made in the momentum transfer variable $\vec{k}$.

The exact form of the quark-antiquark interaction in QCD is also unclear in the case where one or more light quarks are involved. Rather than being a simple relativistic extrapolation of heavy quark physics [16], the interaction between light quarks is likely to involve the instanton induced interaction [24, 25, 26, 27, 33]. In view of this, while the one-gluon exchange + confinement ansatz for the $Q\bar{q}$ system is still used in the calculations, the instanton induced interaction along with its implications is discussed. Throughout this paper, common practice in high energy physics will be adhered to by using "natural units", i.e. $\hbar c = 1$. Thus no factors $\hbar$ or c will appear in the expressions. This is also helpful for the numerical methods used in solving the BSLT equation.

This paper is structured as follows: In section 2 the Blankenbecler-Sugar quasipotential reduction along with the BSLT equation is described. Section 3 presents expressions for the OGE and confining interactions in the BSLT formalism. This section also includes a discussion of the instanton induced interaction for heavy-light mesons. In section 4 the numerical methods used in solving the BSLT equation are discussed, and in section 5, the results are presented and compared to experimental data and other recent work [15] on the subject. Finally section 6 contains a discussion of the problems encountered and comments on future outlook.

2 The Blankenbecler-Sugar equation

This work deals with the system formed of two quarks, which in general may have unequal mass, with masses that are sufficiently low to make a non-relativistic treatment unreliable. This is evidently the case for heavy-light quarkonia, since the velocity of the light quark in those systems is close to that of light. Ideally, when treating such systems, the appropriate way to proceed would be to solve the Bethe-Salpeter (BS) equation for the field-theoretic T-matrix, defined as the latter (interaction) part of the S-matrix [5]:

$$S_{fi} = \delta_{fi} + i(2\pi)^4\,\delta(P_f - P_i)\sqrt{\frac{m^4}{(2\pi)^{12}E_{p'_Q}\,E_{p'_{\bar{q}}}\,E_{p_Q}\,E_{p_{\bar{q}}}}}\,M_{fi}, \tag{1}$$

where the deltafunction guarantees 4-momentum conservation. The field-theoretic scattering amplitude M is then defined through

$$M_{fi} = \bar{u}(p'_Q)\bar{u}(p'_{\bar{q}})\,M\,u(p_Q)u(p_{\bar{q}}). \tag{2}$$

Since the antiquark here has positive energy, it may be described by u spinors. The Bethe-Salpeter equation for M is then formally written as [2]

$$M = V - i\int \frac{d^4k}{(2\pi)^4}\,V\,G\,M, \tag{3}$$

where V is an interaction kernel of irreducible diagrams, for example one-gluon exchange (OGE), and G denotes the Green's function. In this case, G is the relativistic two-particle propagator, which may be obtained from the single particle free-fermion propagators as [35]

$$G \;=\; S_F^Q\,S_F^{\bar{q}}\,, \quad S_F = \frac{\gamma_\mu p^\mu + m}{p^2 - m^2 + i\epsilon}. \tag{4}$$

For the sake of simplicity, the case of equal quark and antiquark masses is considered first. In the $Q\bar{q}$ center-of-mass frame, the relevant 4-momenta are defined as in Fig. 1:

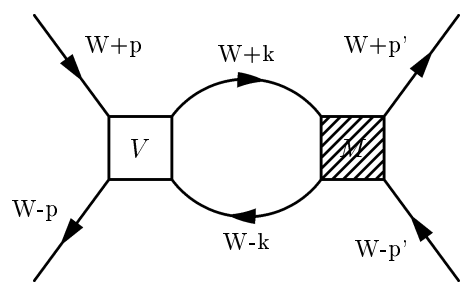

Figure 1: Graphical representation of the second term on the right-hand side of the Bethe-Salpeter equation, with the four-vectors $p = (\vec{p}, 0)$, $k = (\vec{k}, k_0)$, $W = (\vec{0}, w)$ and $w = 1/2 \times$ incoming energy.

In this representation, the propagator in eq. (4) can be expressed as

$$G = S_F^Q(W+k)S_F^{\bar{q}}(W-k) = \frac{(\gamma_\mu^Q(W+k)^\mu + m)(\gamma_\mu^{\bar{q}}(W-k)^\mu + m)}{((W+k)^2 - m^2 + i\epsilon)((W-k)^2 - m^2 + i\epsilon)}. \tag{5}$$

However, because of the difficulties [2] associated with numerical solution of the full Bethe-Salpeter equation for a system with the same degree of complexity as heavy-light quarkonia, a more convenient approach is to use some form of quasipotential reduction. The aim is to convert the

4-dimensional BS equation to a three-dimensional form, which can be treated by standard techniques developed for the solution of the Lippmann-Schwinger (LS) and Schrödinger equations. Several different quasipotential reductions of the BS equation have been developed over the years. In this work the method of Blankenbecler and Sugar in ref. [2], modified to take into account the fermion projection operators, is used. In this formalism the two-particle fermion propagator G is replaced by a simpler nonrelativistic propagator g which satisfies a relativistic (elastic) unitarity relation. One can define

$$F = -i \int \frac{d^4k}{(2\pi)^4} V\, G\, M, \tag{6}$$

and demand that the new propagator g should give rise to the same discontinuity ΔF across the physical two-particle cut. The discontinuity can be evaluated, in accordance with the Cutcosky rules [37], by replacing the denominator factors in eq. (5) with delta functions, giving

$$\begin{aligned} \Delta F &= i \int \frac{d^4k}{(2\pi)^2} V [\gamma_\mu^Q (W+k)^\mu + m][\gamma_\mu^{\bar{q}} (W-k)^\mu + m]\, M \\ &\quad \delta[(W+k)^2 - m^2]\ \delta[(W-k)^2 - m^2]. \end{aligned} \tag{7}$$

The choice originally explored in [2] that gives rise to the same discontinuity ΔF, with exception of the fermion projection operators used here, is to use the following form for the BSLT equation propagator g:

$$\begin{aligned} g &= 2\pi i \int_0^\infty \frac{dw'^{\,2}}{w'^{\,2} - w^2 + i\epsilon} [\gamma_\mu^Q (w'+k)^\mu + m][\gamma_\mu^{\bar{q}} (w'-k)^\mu + m] \\ &\quad \delta[(w'+k)^2 - m^2]\ \delta[(w'-k)^2 - m^2] \end{aligned} \tag{8}$$

In this expression, the w'-integration may be carried out analytically in the CM-frame, producing the following result [2, 7]:

$$g = 2\pi i\, \delta(k_0) \frac{(\gamma_0^Q E_k - \vec{\gamma}^Q \cdot \vec{k} + m)(\gamma_0^{\bar{q}} E_k + \vec{\gamma}^{\bar{q}} \cdot \vec{k} + m)}{4E_k(\vec{k}^{\,2} - \vec{q}^{\,2} + i\epsilon)}. \tag{9}$$

Here the notations $E_k = \sqrt{\vec{k}^{\,2} + m^2}$ and $w = \sqrt{\vec{q}^{\,2} + m^2}$ have been used. k_0 denotes the time-component of the four-vector k. The Blankenbecler-Sugar equation (BSLT) is then defined in the same way as the BS equation,

$$M = U + U\, g\, M, \tag{10}$$

where a four-dimensional integral in understood over the second term on the right-hand side. The quantity U replacing the interaction kernel V is called the quasipotential. The quasipotential U is generated from V by the propagator $G - g$, giving

$$U = V + V\,(G - g)\, U. \tag{11}$$

Essentially this procedure amounts to rewriting the BS equation as two equations. The first one is three-dimensional and resembles the Lippmann-Schwinger equation, while the second one is a defining equation for the quasipotential U. Since, generally $\Delta F(s) = 2i\ \mathrm{Im}\ F(s + i\epsilon)$ [37], the demand that the propagators G and g have the same discontinuity ΔF leads to the fact that $G - g$ lacks a physical two-particle cut, and is therefore expected to have a weak energy dependence. This is equivalent to stating that

$$\mathrm{Im}\,[V\, G\, U] = \mathrm{Im}\,[V\, g\, U]. \tag{12}$$

Since V is real, this restriction forces the quasipotential U to be real as well, but places no additional restrictions on the real part of U, and thus one may add any expression to g as long as g has the same ΔF as G. Consequently several different forms for g have been proposed, particularly in [8] and [9]. These include various combinations of the projection operators for positive and negative energy states. In this work, it has been decided to use the form of eq. (9), primarily because it leads to a potential with simple analytic properties. Clearly, the simplest approximation, which is used in [2] is to proceed by setting $U \approx V$, which is also done in this work. The great simplification inherent in eq. (9) is the appearance of a deltafunction in k_0 which reduces the BS equation into a 3-dimensional form. In this context, one may note that an additional feature of the Blankenbecler-Sugar reduction is that the appearance of the deltafunction also eliminates the possibility of having gauge-dependent retardation contributions to the effective interaction. If one defines the Dirac spinor matrix

$$\Lambda^+ = \frac{\gamma_\mu k^\mu + m}{2m} = \sum_\sigma u_{\vec{k}\sigma}\bar{u}_{\vec{k}\sigma}, \tag{13}$$

that acts as a projection operator for positive energy states, and

$$\Lambda^- = -\frac{\gamma_\mu k^\mu - m}{2m} = \sum_\sigma v_{\vec{k}\sigma}\bar{v}_{\vec{k}\sigma} \tag{14}$$

which is a corresponding operator for negative energy states, then it becomes possible to rewrite the propagator g as

$$g = 2\pi i\,\delta(k_0)\frac{m^2}{E_k}\frac{\Lambda_Q^+\Lambda_{\bar{q}}^+}{\vec{k}^{\,2} - \vec{q}^{\,2} + i\epsilon}. \tag{15}$$

This form of the BSLT propagator makes a transformation to a Pauli-spinor representation defined by

$$M, V \rightarrow \left\langle \bar{u}^Q(\vec{p}\,')\bar{u}^{\bar{q}}(-\vec{p}\,')|M, V(\vec{p}\,', \vec{p})|u^Q(\vec{p})u^{\bar{q}}(-\vec{p})\right\rangle \tag{16}$$

useful. In this way a field-theoretical form for the BSLT equation, which is formally equivalent to that of the Lippmann-Schwinger equation, is obtained. The most obvious difference is the appearance of the extra factor m/E, which is characteristic of the BSLT equation. This is also often referred to as "Minimal Relativity" in the literature. Thus, with the aid of eqs. (15) and (16) this form of the BSLT equation may be written as

$$M = V + \int \frac{d^3k}{(2\pi)^3}\,\frac{m^2}{E_k}\,V\,\frac{1}{\vec{k}^{\,2} - \vec{q}^{\,2} + i\epsilon}\,M. \tag{17}$$

If one then wishes to express the BSLT equation in the conventional quantum mechanical framework, one has to take into account a sign difference in the definition of the S-matrix. This is conveniently accomplished by changing the sign of both the scattering amplitude M and the interaction V in eq. (17). At this point it is also desirable to generalize the BSLT equation to the case of unequal quark masses. These modifications are relatively insignificant and affect only the "Minimal Relativity" factors, giving

$$T(\vec{p}\,', \vec{p}) = V(\vec{p}\,', \vec{p}) - \int \frac{d^3k}{(2\pi)^3}\frac{Mm}{W(\vec{k})}V(\vec{p}\,', \vec{k})\frac{1}{\vec{k}^{\,2} - \vec{q}^{\,2} + i\epsilon}T(\vec{k}, \vec{p}), \tag{18}$$

where T represents the BSLT scattering amplitude, and V denotes the BSLT interaction. The function $W(\vec{k})$ is defined as $(E_Q(\vec{k}) + E_{\bar{q}}(\vec{k}))/2$, in accordance with Fig. 1. It is evident that eq. (18) reduces straightforwardly to the case of equal quark and antiquark masses. In this paper the BSLT equation will be solved by converting it into a differential equation that resembles the Schrödinger equation. For this purpose, it is convenient to make the redefinition

$$\mathcal{T}(\vec{p}\,',\vec{p}) = \sqrt{\frac{M+m}{2W(\vec{p}\,')}}\,T(\vec{p}\,',\vec{p})\sqrt{\frac{M+m}{2W(\vec{p})}}, \tag{19}$$

for the scattering amplitude, and

$$\mathcal{V}(\vec{p}\,',\vec{p}) = \sqrt{\frac{M+m}{2W(\vec{p}\,')}}\,V(\vec{p}\,',\vec{p})\sqrt{\frac{M+m}{2W(\vec{p})}}. \tag{20}$$

for the potential. These redefinitions have the effect of removing the extra "Minimal Relativity" factor from eq. (18), giving

$$\mathcal{T}(\vec{p}\,',\vec{p}) = \mathcal{V}(\vec{p}\,',\vec{p}) - \int \frac{d^3k}{(2\pi)^3}\mathcal{V}(\vec{p}\,',\vec{k})\frac{2\mu}{\vec{k}^{\,2} - \vec{q}^{\,2} + i\epsilon}\mathcal{T}(\vec{k},\vec{p}). \tag{21}$$

In the above equation, μ stands for the usual two-particle reduced mass. Since this form of the BSLT equation is completely analogous to the LS equation as obtained from the nonrelativistic Schrödinger equation, it may be identified as a differential eigenvalue equation of Schrödinger type, where the potential V corresponds to $\mathcal{V}$ in eq. (20). The BSLT equation may thus be recast in coordinate space as

$$\left[-\frac{\vec{\nabla}^{\,2}}{2\mu} + \mathcal{V}(\vec{r},\vec{P})\right]\Psi_{\mathrm{nlm}}(\vec{r}) = \varepsilon\Psi_{\mathrm{nlm}}(\vec{r}). \tag{22}$$

The advantage of eq. (22) is that while it retains the conventional quantum mechanical operator structure, it still takes full account of the relativistic kinetic energy. Although nonlocal from the start, the potential $\mathcal{V}(\vec{r},\vec{P})$ may, for calculational purposes, be interpreted as the normal Schrödinger equation potential, remembering to modify it according to eq. (20). These square root factors make $V(\vec{r},\vec{P})$ more nonlocal and have an extra dampening effect. The relativistic treatment of the kinetic energy manifests itself in the eigenvalue ε of eq. (22). In the Schrödinger equation this would correspond to the excitation energy $E - M - m$, where E denotes the total energy of the $Q\bar{q}$ state. Since $\vec{q}$ in eq. (9) is on the mass shell, it follows that ε is given by

$$\varepsilon = \frac{\vec{q}^{\,2}}{2\mu} = \frac{\left[E^2 - (M+m)^2\right]\left[E^2 - (M-m)^2\right]}{8\mu E^2}. \tag{23}$$

It is evident that q may be viewed as the momentum imparted to the quarks in the CM-frame when the meson "decays" into its constituent quarks, as in the external lines in Fig. 1. In the case of equal quark and antiquark masses, this expression reduces to

$$\varepsilon_{M=m} = \frac{E^2 - 4m^2}{4m}, \tag{24}$$

which is the form most often encountered in the literature. Thus the main and most important advantage of the BSLT equation over the conventional Schrödinger formalism is the completely relativistic treatment of the two-particle kinetic energy operator, which turns out to be extremely important for a realistic description of the heavy-light mesons. The main disadvantage is that the operator structure of eq. (22) precludes an exact treatment of nonlocal effects. It is finally worth noting that the expression for ε is not entirely unexpected, and might have been invented without all the above analysis. After all, the main obstacle to obtaining realistic spectra for lighter mesons using the nonrelativistic Schrödinger equation is the unrealistic quadratic behavior of the kinetic energy. This being the case, an additional advantage of the BSLT equation over the "relativized" Schrödinger equation is that the square root factors $\sqrt{m/E}$ provide direct contact with the conventional field-theoretical Bethe-Salpeter formalism.

3 The Interaction Hamiltonian for $Q\bar{q}$ systems

For heavy quarkonia, the most important components of the interaction between quarks are the one-gluon exchange (OGE) interaction, which couples as a vector invariant, and the confining interaction, which will be assumed on the basis of compelling evidence, to couple as a scalar invariant. These can be understood in terms of the simple Feynman diagrams in Fig. 2:

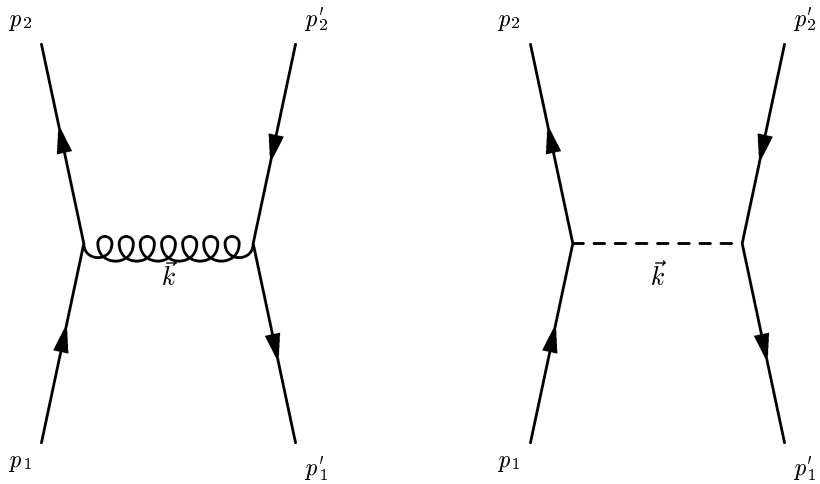

Figure 2: Feynman diagrams describing the processes considered in this paper. The following labeling convention for the four-vectors has been used: $p_1 = (\vec{p}, E_Q)$, $p_2 = (\vec{p}\,', E_Q')$, $p_1' = (-\vec{p}, E_{\bar{q}})$, $p_2' = (-\vec{p}\,', E_{\bar{q}}')$. Note that $E_Q = \sqrt{M^2 + \vec{p}^{\,2}}$, $E_Q' = \sqrt{M^2 + \vec{p}^{\,\prime 2}}$, $E_{\bar{q}} = \sqrt{m^2 + \vec{p}^{\,2}}$, and $E_{\bar{q}}' = \sqrt{m^2 + \vec{p}^{\,\prime 2}}$.

For the confining interaction, it will be assumed that it couples as a Lorentz scalar. In that case, the confining interaction may be expressed in momentum space in the following form, where $\vec{k}$ denotes the relative momentum [34]:

$$V_c(\vec{p}, \vec{p}\,') = \bar{\psi}(p_2)\, \mathbb{1}\, \psi(p_1) V_c(\vec{k})\, \bar{\psi}(p_2')\, \mathbb{1}\, \psi(p_1'). \tag{25}$$

The Dirac spinors ψ are defined as [34]

$$\psi(p) = \sqrt{\frac{M}{E_Q}} u(p) e^{ip\cdot x}, \tag{26}$$

where the factor $\sqrt{M/E_Q}$, which counteracts the Lorentz contraction of the volume element, guarantees that the integral over the charge density ρ

$$\int d^3 r\, \bar{\psi} \gamma_0 \psi, \tag{27}$$

remains invariant. The adjoint spinor $\bar{\psi}$ is defined as $\bar{u}(p) = u^\dagger(p)\gamma_0$. Throughout, the symbol $\mathbb{1}$ will denote the unit matrix. $V_c(\vec{k})$ denotes the dynamical form of the confining interaction in momentum space. More to the point, V_c is an expression in momentum space that corresponds to cr, a linearly rising potential in coordinate space. Since, strictly speaking, the Fourier transform of

such a potential cannot exist other than as a boundary value, the coordinate space representation will be adhered to throughout the calculations. The spinors $u(p)$ are defined as

$$u(p_1) = \sqrt{\frac{E_Q + M}{2M}} \begin{pmatrix} 1 \\ \frac{\vec{\sigma}_Q \cdot \vec{p}}{E_Q + M} \end{pmatrix} \xi, \tag{28}$$

$$\bar{u}(p_2) = \sqrt{\frac{E'_Q + M}{2M}} \left(1, \; -\frac{\vec{\sigma}_Q \cdot \vec{p}\,'}{E'_Q + M} \right) \xi^\dagger, \tag{29}$$

for the heavy quark Q, and

$$u(p'_1) = \sqrt{\frac{E_{\bar{q}} + m}{2m}} \begin{pmatrix} 1 \\ -\frac{\vec{\sigma}_{\bar{q}} \cdot \vec{p}}{E_{\bar{q}} + m} \end{pmatrix} \xi, \tag{30}$$

$$\bar{u}(p'_2) = \sqrt{\frac{E'_{\bar{q}} + m}{2m}} \left(1, \; \frac{\vec{\sigma}_{\bar{q}} \cdot \vec{p}\,'}{E'_{\bar{q}} + m} \right) \xi^\dagger \tag{31}$$

for the light antiquark $\bar{q}$. In order to simplify the notation, the antiquark is described in terms of the positive energy spinors u. In these expressions the normalization $\bar{u}(p)u(p) = 1$ has been employed, ensuring that the normalization prescription is Lorentz invariant. The momenta, spins and energies are labeled according to the notation in Fig. (2). The calculations are greatly facilitated by use of the identity

$$\vec{\sigma} \cdot \vec{a} \;\; \vec{\sigma} \cdot \vec{b} = \vec{a} \cdot \vec{b} + i\vec{\sigma} \cdot \vec{a} \times \vec{b}, \tag{32}$$

by which the product of the spinors for the heavy quark Q in eq. (25) may be expressed as

$$\bar{\psi}(p_2)\, 1\, \psi(p_1) = \sqrt{\frac{E_Q + M}{2E_Q}} \sqrt{\frac{E'_Q + M}{2E'_Q}} \left(1 - \frac{\vec{p}\,' \cdot \vec{p} + i\vec{\sigma}_Q \cdot (\vec{p}\,' \times \vec{p})}{(E'_Q + M)(E_Q + M)} \right). \tag{33}$$

Expressions of this type are often referred to as Dirac bispinors. The corresponding bispinor for the antiquark $\bar{q}$ may be constructed in a similar way by combining eqs. (30) and (31). In the case of the OGE interaction, the coupling structure is somewhat more complicated, as the fact that it couples as a vector invariant has to be taken into account. The proper form of this interaction in momentum space can be obtained as [34, 36]

$$V_g(\vec{p}, \vec{p}\,') = \bar{\psi}(p_2)\, \gamma_Q^\mu \; \psi(p_1) V_g(\vec{k}) \; \bar{\psi}(p'_2)\, \gamma_{\bar{q}}^\nu \; \psi(p'_1), \tag{34}$$

where the Dirac gamma-matrices γ^μ have been introduced. It is evident that the form of eq. (34) is similar to that of eq. (25), only now instead of the unity matrices the Dirac γ-matrices have to be sandwiched between the spinors. Since V_g contains a factor $g_{\mu\nu}$, it follows that the bispinors in eq. (34) may be combined into a single expression. The usual way to proceed is to split up eq. (34) into the so-called current- and charge-coupling (spatial) terms. The current-coupling term $\bar{\psi}(p_2)\, \gamma^\mu \; \psi(p_1)$ with $\mu = 1, 2, 3$ can be expressed as

$$\bar{\psi}(p_2)\, \vec{\gamma}^{\,Q} \; \psi(p_1) = \sqrt{\frac{E_Q + M}{2E_Q}} \sqrt{\frac{E'_Q + M}{2E'_Q}} \left(1, \; -\frac{\vec{\sigma}_Q \cdot \vec{p}\,'}{E'_Q + M} \right) \begin{bmatrix} 0 & \vec{\sigma}_Q \\ -\vec{\sigma}_Q & 0 \end{bmatrix} \begin{pmatrix} 1 \\ \frac{\vec{\sigma}_Q \cdot \vec{p}}{E_Q + M} \end{pmatrix}, \tag{35}$$

where the appropriate expression for the other quark can be obtained by switching the spinors and quark masses accordingly. After multiplication and application of eq. (32), the current-coupling term may be recast in the following form,

$$\bar{\psi}(p_2)\,\vec{\gamma}^{\,Q}\,\psi(p_1) = \sqrt{\frac{E_Q+M}{2E_Q}}\sqrt{\frac{E'_Q+M}{2E'_Q}}\left(\frac{\vec{p}-i\vec{\sigma}_Q\times\vec{p}}{E_Q+M}+\frac{\vec{p}\,'+i\vec{\sigma}_Q\times\vec{p}\,'}{E'_Q+M}\right) \tag{36}$$

for the heavy quark Q, and

$$\bar{\psi}(p'_2)\,\vec{\gamma}^{\,\bar{q}}\,\psi(p'_1) = -\sqrt{\frac{E_{\bar{q}}+m}{2E_{\bar{q}}}}\sqrt{\frac{E'_{\bar{q}}+m}{2E'_{\bar{q}}}}\left(\frac{\vec{p}-i\vec{\sigma}_{\bar{q}}\times\vec{p}}{E_{\bar{q}}+m}+\frac{\vec{p}\,'+i\vec{\sigma}_{\bar{q}}\times\vec{p}\,'}{E'_{\bar{q}}+m}\right) \tag{37}$$

for the light antiquark $\bar{q}$. Here the vector nature of these terms can be clearly seen. If the quark momenta are small, the current-coupling term is negligible. The remaining term, the charge-coupling term is dominant and remains in the nonrelativistic limit. This scalar term can be expressed as follows,

$$\bar{\psi}(p_2)\,\gamma_0^{Q}\,\psi(p_1) = \sqrt{\frac{E_Q+M}{2E_Q}}\sqrt{\frac{E'_Q+M}{2E'_Q}}\left(1,\ -\frac{\vec{\sigma}_Q\cdot\vec{p}\,'}{E'_Q+M}\right)\begin{bmatrix}1 & 0\\ 0 & -1\end{bmatrix}\begin{pmatrix}1\\ \frac{\vec{\sigma}_Q\cdot\vec{p}}{E_Q+M}\end{pmatrix} \tag{38}$$

where the corresponding expression for the other quark can again be obtained as in eqs. (33) and (36). The structure of this term is similar to that obtained for the scalar interaction, the only difference being the sign change imparted by γ_0. Thus the following expression for the charge coupling term is obtained:

$$\bar{\psi}(p_2)\,\gamma_0^{Q}\,\psi(p_1) = \sqrt{\frac{E_Q+M}{2E_Q}}\sqrt{\frac{E'_Q+M}{2E'_Q}}\left(1+\frac{\vec{p}\,'\cdot\vec{p}+i\vec{\sigma}_Q\cdot(\vec{p}\,'\times\vec{p})}{(E'_Q+M)(E_Q+M)}\right). \tag{39}$$

Since it is of interest to develop an interaction model suitable for the BSLT equation, the expressions obtained so far have to be modified by the BSLT factors from eq. (20). Thus the BSLT potential in momentum space can be obtained as

$$\mathcal{V}_{\rm BSLT}(\vec{p}\,',\vec{p}) = \sqrt{\frac{M+m}{2W(\vec{p}\,')}}V(\vec{p}\,',\vec{p})\sqrt{\frac{M+m}{2W(\vec{p})}}, \tag{40}$$

where the appearance of the additional dampening $\sqrt{m/E}$ factors into the interaction is again noted. This effect vanishes only when both quark and antiquark are infinitely massive, in which limit the BSLT equation also approaches the familiar nonrelativistic Schrödinger equation. At this point, one needs to establish the form of V_g in momentum space. By analogy with QED, the form of the one-gluon exchange interaction in QCD can be obtained in terms of the momentum transfer (relative momentum) $\vec{k}$ as [36]:

$$V_g(\vec{k}) = \frac{g_s^2}{\vec{k}^{\,2}}g_{\mu\nu}T_Q\cdot T_{\bar{q}}. \tag{41}$$

Here the factors T_i denote the generators of SU(3) theory. These are defined in terms of the Gell-Mann λ-matrices, giving in the case of a meson [16]

$$\langle T_Q\cdot T_{\bar{q}}\rangle = \langle\lambda_Q\cdot\lambda_{\bar{q}}\rangle/4 = -4/3. \tag{42}$$

This amounts to considering all possible color combinations in the diagram in Fig. 2. As noted earlier, the factor $g_{\mu\nu}$ is conveniently absorbed into eq. (34), and the usual definition of the strong coupling strength is $\alpha_s = g_s^2/4\pi$. This results in the form

$$V_g(\vec{k}) = -\frac{16\pi}{3}\frac{\alpha_s(\vec{k}^{\,2})}{\vec{k}^{\,2}} \tag{43}$$

for the OGE interaction in momentum space. If the strength of the strong coupling α_s is taken to be constant, eq. (43) becomes a Coulombic potential in coordinate space, provided that the constituent quarks are sufficiently heavy so that relativistic effects can be neglected. In this work α_s will not be taken to be constant. Instead, the parametrization given by eq. (86) is used. As mentioned earlier, the form of the confining interaction in momentum space, $V_c(\vec{k})$ is more problematic. If one proceeds by replacing the linear potential by the form

$$V_c(r) = cr\, e^{-\lambda r}, \tag{44}$$

in coordinate space, then it becomes possible to Fourier transform the confining interaction to momentum space by

$$V_c(k) = \int_0^\infty d^3r\, e^{-i\vec{k}\cdot\vec{r}}\, V_c(r), \tag{45}$$

since it is no longer infinitely rising. This form has been used earlier, for example in ref. [13]. The Fourier transform of eq. (44) then becomes

$$V_c(\vec{k}) = 8\pi c \left(\frac{4\lambda^2}{(\lambda^2+k^2)^3} - \frac{1}{(\lambda^2+k^2)^2} \right), \tag{46}$$

where the intention is to take the limit as $\lambda \to 0$. This, however, renders the inverse Fourier transform divergent. Thus more elaborate techniques are required and these are discussed further in section 3.1. Since the expressions for the charge- and current coupling contributions to the OGE interaction have been worked out, the complete OGE interaction in momentum space may be expressed as

$$\begin{aligned}
\mathcal{V}_g(\vec{p}\,',\vec{p}) \;=\; & \sqrt{\frac{M+m}{E_Q+E_{\bar{q}}}}\sqrt{\frac{M+m}{E'_Q+E'_{\bar{q}}}}\sqrt{\frac{E_Q+M}{2E_Q}}\sqrt{\frac{E'_Q+M}{2E'_Q}}\sqrt{\frac{E'_{\bar{q}}+m}{2E'_{\bar{q}}}}\sqrt{\frac{E_{\bar{q}}+m}{2E_{\bar{q}}}}\, V_g(\vec{k}) \\
& \left[\left(\frac{\vec{p} - i\vec{\sigma}_Q \times \vec{p}}{E_Q+M} + \frac{\vec{p}\,' + i\vec{\sigma}_Q \times \vec{p}\,'}{E'_Q+M} \right) \left(\frac{\vec{p} - i\vec{\sigma}_{\bar{q}} \times \vec{p}}{E_{\bar{q}}+m} + \frac{\vec{p}\,' + i\vec{\sigma}_{\bar{q}} \times \vec{p}\,'}{E'_{\bar{q}}+m} \right) \right. \\
& \left. + \left(1 + \frac{\vec{p}\,'\cdot\vec{p} + i\vec{\sigma}_Q \cdot (\vec{p}\,' \times \vec{p})}{(E'_Q+M)(E_Q+M)} \right) \left(1 + \frac{\vec{p}\,'\cdot\vec{p} + i\vec{\sigma}_{\bar{q}} \cdot (\vec{p}\,' \times \vec{p})}{(E'_{\bar{q}}+m)(E_{\bar{q}}+m)} \right) \right],
\end{aligned} \tag{47}$$

where $V_g(\vec{k})$ is taken to be as in eq. (43). Similarly, one can obtain the complete expression for the scalar confining interaction in momentum space, after multiplication with the BSLT square root factors in (40):

$$\begin{aligned}
\mathcal{V}_c(\vec{p}\,',\vec{p}) \;=\; & \sqrt{\frac{M+m}{E_Q+E_{\bar{q}}}}\sqrt{\frac{M+m}{E'_Q+E'_{\bar{q}}}}\sqrt{\frac{E_Q+M}{2E_Q}}\sqrt{\frac{E'_Q+M}{2E'_Q}}\sqrt{\frac{E'_{\bar{q}}+m}{2E'_{\bar{q}}}}\sqrt{\frac{E_{\bar{q}}+m}{2E_{\bar{q}}}}\, V_c(\vec{k}) \\
& \left(1 - \frac{\vec{p}\,'\cdot\vec{p} + i\vec{\sigma}_Q \cdot (\vec{p}\,' \times \vec{p})}{(E'_Q+M)(E_Q+M)} \right) \left(1 - \frac{\vec{p}\,'\cdot\vec{p} + i\vec{\sigma}_{\bar{q}} \cdot (\vec{p}\,' \times \vec{p})}{(E'_{\bar{q}}+m)(E_{\bar{q}}+m)} \right).
\end{aligned} \tag{48}$$

In these expressions, the spin-independent part is parametrized in terms of the operator $\vec{p}\,'\cdot\vec{p}$. The spin-dependent part that is linear in $\vec{\sigma}_\mu$ can be conveniently broken up into parts that are best expressed in terms of the potential operators Ω. For example the spin-orbit interaction can be broken up into symmetric and antisymmetric parts that are proportional to

$$\Omega_{\rm SLS} = \frac{i}{2}(\vec{\sigma}_Q + \vec{\sigma}_{\bar{q}}) \cdot \vec{p}\,' \times \vec{p}, \tag{49}$$

for the standard symmetric spin-orbit interaction, and

$$\Omega_{\rm ALS} = \frac{i}{2}(\vec{\sigma}_Q - \vec{\sigma}_{\bar{q}}) \cdot \vec{p}\,' \times \vec{p} \tag{50}$$

for the antisymmetric interaction, which vanishes for equal mass quarkonia. This operator also has no diagonal matrix elements, and contributes only in second order perturbation theory. These spin-orbit interactions appear both for the confining and OGE interactions. In case of the confining interaction, the symmetric part is sometimes referred to as "Thomas-precession". The remaining potential operators appear only for a vector interaction, since they originate in the current-coupling terms. Consequently they do not contribute to the scalar confining interaction. These can be summarized by

$$\Omega_{\rm T} = (\vec{\sigma}_Q \cdot \vec{\sigma}_{\bar{q}})\ \vec{k}^{\,2} - 3(\vec{\sigma}_Q \cdot \vec{k})(\vec{\sigma}_{\bar{q}} \cdot \vec{k}), \tag{51}$$

which is referred to as the tensor interaction, and

$$\Omega_{\rm SS} = \vec{\sigma}_Q \cdot \vec{\sigma}_{\bar{q}}\ \vec{k}^{\,2}, \tag{52}$$

which describes the spin-spin interaction between the quarks. The tensor interaction does not contribute to the hyperfine structure for S-states, since it averages to zero for radially symmetric states. In these expressions, $\vec{k} = \vec{p}\,' - \vec{p}$, the relative momentum. This momentum variable becomes useful, as it is convenient to go to the center-of-momentum system (cms), which is defined by

$$\vec{k} = \vec{p}\,' - \vec{p}, \qquad \vec{P} = \frac{\vec{p}\,' + \vec{p}}{2}, \tag{53}$$

where $\vec{k}$ denotes the relative momentum and $\vec{P}$ the total momentum. This leads to the substitutions

$$\vec{p} = \vec{P} - \frac{\vec{k}}{2}, \qquad \vec{p}\,' = \vec{P} + \frac{\vec{k}}{2}. \tag{54}$$

The cms momenta are natural and convenient, since $\vec{k}$ corresponds to the radial coordinate r in the CM-system, and can be included in $\mathcal{V}(r)$ by Fourier transformation. The other variable, $\vec{P}$, models the nonlocality in the potential and corresponds to the kinetic energy operator in the BSLT equation. Unfortunately, in coordinate space the treatment is restricted to an expansion up to second order in $\vec{P}$. However, even if one expands the interaction to second order in $\vec{P}$, there still remains the possibility to treat that term exactly in $\vec{k}$, and therefore this treatment in still much more realistic than if one had expanded in $\vec{k}$ as well. In the same manner, the various spin-dependent contributions can be treated exactly in $\vec{k}$. In principle, they could also be treated exactly to order $\vec{P}^2$, but since these contributions are of order m^{-4}, they are not considered here. When computing the central and spin-dependent components from eqs. (47) and (48), the variables $\vec{P}$ and $\vec{k}$ appear in the following combinations:

$$\vec{p}\,' \cdot \vec{p} = \vec{P}^{\,2} - \frac{\vec{k}^{\,2}}{4} \tag{55}$$

in the spin-independent part of the interaction, and

$$\vec{p}\,' \times \vec{p} = \vec{k} \times \vec{P} \tag{56}$$

in the spin-dependent part. It then follows that in coordinate space, the symmetric spin-orbit interaction is proportional to

$$\mathcal{V}_{LS} \sim \left\langle \vec{S} \cdot \vec{L} \right\rangle \frac{1}{r}\frac{\partial}{\partial r}, \tag{57}$$

and the quadratic spin-orbit interaction to

$$\mathcal{V}_Q \sim \langle Q_{12} \rangle \frac{1}{r} \frac{\partial}{\partial r} \frac{1}{r} \frac{\partial}{\partial r}. \tag{58}$$

In these expressions, the spin-orbit coefficient is defined as

$$\vec{S} \cdot \vec{L} = \frac{1}{2} (\vec{\sigma}_Q + \vec{\sigma}_{\bar{q}}) \cdot \vec{L} \ , \tag{59}$$

and the quadratic spin-orbit coefficient as

$$Q_{12} = (\vec{\sigma}_Q \cdot \vec{L}\, \vec{\sigma}_{\bar{q}} \cdot \vec{L} + \vec{\sigma}_{\bar{q}} \cdot \vec{L}\, \vec{\sigma}_Q \cdot \vec{L})/2 \ , \tag{60}$$

where $\vec{L} = \vec{r} \times \vec{P}$. The quadratic spin-orbit interaction arises from the term in eqs. (47) and (48) that is quadratic in $\vec{\sigma}_\mu$. The expression for the tensor interaction in coordinate space is obtained as

$$S_{12} = 3(\vec{\sigma}_Q \cdot \hat{r})(\vec{\sigma}_{\bar{q}} \cdot \hat{r}) - \vec{\sigma}_Q \cdot \vec{\sigma}_{\bar{q}}. \tag{61}$$

Since the intention in this work is not to treat the BSLT equation exactly in momentum space, a choice has to be made concerning the degree of approximation to be applied. One is already compelled to expand the potential to order $\vec{P}^{\,2}$ from the start, since the BSLT equation has been converted into a differential equation in coordinate space. The main advantage here over previous work is an unapproximated treatment in $\vec{k}$ for the OGE interaction. The obtained nonstatic expressions are finally transferred into coordinate space by inverse Fourier transformation as

$$\mathcal{V}(\vec{r}, \vec{P}) = \int \frac{d^3k}{(2\pi)^3} \mathcal{V}(\vec{k}, \vec{P}) e^{i\vec{k}\cdot\vec{r}}, \tag{62}$$

giving a potential in coordinate space which, in general, may depend on both $\vec{r}$ and $\vec{P}$.

3.1 The confining interaction

A very important component of the $Q\bar{q}$ interaction is the confining interaction. Sadly, this is also one of the least understood phenomena in high-energy physics. Therefore, it is instructive to carefully analyze the various phenomena in which the character of the confining interaction may manifest itself. A long standing and important problem is whether the coupling structure of confinement is of scalar or vector nature. Until recently, the strongest evidence for a scalar confining interaction has been the observed spin-orbit structure of the P-states in heavy quarkonia. The OGE interaction has a large spin-orbit part which can be largely cancelled by the spin-orbit contribution from confinement, provided that it couples as a scalar. This statement has recently been challenged, particularly in ref. [14], where a mixture of scalar and vector confinement with an anticonfining scalar part is used. There, the scalar appearance of the spin-orbit splittings in charmonium is generated by a construction, which gives confinement of scalar nature for the spin-dependent interaction while assuring that the spin-independent part is of vector nature. In that model, inverted spin-orbit splittings are found in many cases concerning the heavy-light mesons. Recent experimental measurements [32] and numerical lattice NRQCD calculations [12] apparently discredit the predictions of the model used in [14], while being in satisfactory agreement with the results obtained here.

However, there is much stronger evidence against an effective vector confining interaction in the observed M1 decay widths of charmonium ($c\bar{c}$). This issue was investigated in ref. [29] by using the Bethe-Salpeter equation with instantaneous interactions. However, the results did not agree satisfactorily with experiment, partly because of an inadequate interaction kernel. In ref. [17] it is shown in the Schrödinger formalism that once the full Dirac structure of the spin-flip magnetic moment of the quark and antiquark is taken into account, in addition to the exchange current contribution that appears if the confining interaction couples as a scalar, the observed M1 decay rates are naturally explained without any need for more elaborate constructions. This two-quark current is required by current conservation with the scalar confining interaction. A similar contribution appears for the axial charge of nucleons in nuclei [20], where it is crucial for agreement with empirical data. In addition it is shown in [17] that a vector interaction can contribute directly to the M1 decay rates only if the quark masses are unequal.

Thus it may be concluded that a vector confining interaction does not contribute to the M1 decay rates of charmonium through an exchange current. In addition, if the nature of the scalar interaction would be anticonfining, as in [14], agreement with the empirical M1 decay rates would be excluded. It should be emphasized that this is so independent of the exact functional form of confinement. Thus the M1 decay rates of heavy quarkonia provide very strong evidence for a scalar confining interaction. It should be stressed that it is very important to use an unapproximated form of the spin-flip magnetic moment operator. If this is expanded to any order in $\vec{p}/m$ unrealistic results will follow, possibly leading to an opposite conclusion about the necessity of the exchange current contribution from the scalar confining interaction. This may be the cause of the opposite conclusion concerning the M1 transitions in [14]. The details of the M1 transition calculations may be found in ref. [28], and the derivation of the exchange current operators is presented in [19].

There are also certain theoretical arguments against a dominant confining interaction of vector nature. In [21] an exact inequality is presented, which involves the static QCD spin-spin and tensor potentials, leading to restrictions on the confining interaction. In particular it is demonstrated that an effective vector interaction can rise at most logarithmically with distance, while there is no problem with OGE. The constraints in [21] are trivially fulfilled by a scalar linear confining interaction. A superposition of scalar and vector confining interactions with positive weights is also ruled out. Further, in [21] it is remarked that a pure vector potential would lead to a Klein paradox.

The exact functional form of the confining interaction, however, is again an essentially open issue. There may be some theoretical grounds on which to expect it to be linear at long range, and numerical lattice calculations [10] suggest that it may be linear at short range. One has to

admit however, that as the confining interaction has quite a large coupling constant, typically ranging between 850-1200 MeV/fm, it is essentially a nonperturbative interaction with large nonlocal contributions. Combining these purely methodological difficulties with the fact that $c\bar{c}$ and $b\bar{b}$ wavefunctions are very compact, it has to be conceded that nonrelativistic calculations alone cannot shed much light on the problem.

However, a harmonic oscillator form for confinement seems to be ruled out by the empirically observed position of the P-states relative to the excited S-states. For quarkonium phenomenology, the question is then mainly whether confinement rises linearly or only logarithmically with quark separation. Calculations of the bottomonium ($b\bar{b}$) spectrum which, because of the massive quarks involved, can be treated in the Schrödinger formalism with some degree of accuracy [17] seem to indicate that good results can indeed be obtained by assuming a linear form for the confining interaction. In ref. [15] the scalar linear confining interaction has also been shown to provide an accurate description of the bottomonium system in a relativistic model.

In view of all these indications, it was decided that a linear form of confinement which couples as a scalar in the spinor representation should be used. This is because that form appears to give favorable and consistent results for both quarkonium spectra and M1 decay rates [15, 17, 18]. To second order in the inverse quark masses this interaction, as calculated from the BSLT formalism, eq. (48), takes the form

$$\begin{aligned} \mathcal{V}_c(r) &= cr\left(1-\frac{3}{2}\frac{\vec{P}^{\,2}}{{m_2}^2}\right)+\frac{c}{4Mmr}-\frac{c}{r}\frac{M^2+m^2}{4M^2m^2}\vec{S}\cdot\vec{L} \\ &\quad +\frac{c}{r}\frac{M^2-m^2}{8M^2m^2}(\vec{\sigma}_Q-\vec{\sigma}_{\bar{q}})\cdot\vec{L}. \end{aligned} \tag{63}$$

Here c is the string tension parameter, the value of which is ~ 1 GeV/fm. The spin–independent Darwin-type term that is proportional to $1/r$ is a consequence of the square root factors in (40). Without those factors the factor 3/2 in the momentum dependent term in first bracket on the right-hand side of eq. (63) would be 1. The terms of second order in the inverse quark masses in (63) are implied by scalar coupling for the confining interaction. As the antisymmetric spin-orbit interaction has no diagonal matrix elements between any of the states in the S- and P-shells, it is not included in this work, since a proper treatment would require the solution of coupled differential equations. The mass coefficient m_2 in the nonlocal correction term is defined as

$$m_2=\sqrt{\frac{3M^2m^2}{M^2+m^2+Mm}}. \tag{64}$$

The term of second order in $\vec{P}$ in the spin-independent term in (63), although formally suppressed by ${M_Q}^2$, is essentially of the same order of magnitude as the leading term cr, even for the $c\bar{c}$ system, as calculations indicate. Even without the factor 3/2 this term is very large in first order perturbation theory for heavy quarkonia [17]. This is not surprising, since the coupling constant (c) of the confining interaction is an order of magnitude larger than that of the OGE interaction (α_s). The problem here is that it is not possible to simply postulate a strong nonperturbative interaction, and then brutally expand it, first in $\vec{k}$, then in inverse powers of m and finally in $\vec{P}$, and still expect the results to be realistic. This is probably so even in a nonperturbative treatment, and is a fact that often appears to have been overlooked, with the motivation that the quarks are "heavy", as the main concern has often only been to obtain wavefunctions for quarkonium states that can be used to predict e.g. decay rates. This is certainly one of the reasons why there is still so much disagreement on the constituent quark masses in various models. Papers that include a large number of "corrections to corrections", no matter how they are treated, should therefore be read with caution, even if they deal with systems composed of heavy quarks only. In view of this, various smaller effects have here been labeled *contributions*, in order to emphasize that they may be of such magnitude that they do not warrant any expansions or approximations, much less a

perturbative treatment. It is important to realize that if one is dealing with an asymptotic series, the correct approach is not to include terms of higher and higher order into the Hamiltonian. A preferable approach is to leave such terms out altogether until an unapproximated treatment is possible. Otherwise, one is forced to truncate the expansion at an arbitrary order, which clearly is not desirable. Indications are that the expansion in $\vec{P}$ is of this nature. The expansion in $\vec{k}$ is not equally problematic for the central part of the confining interaction, since it is primarily a long-range interaction. To further illustrate this point, one may consider the correction term of quartic order, which, as calculated from the BSLT amplitude, takes the following form with exception of the antisymmetric spin-orbit interaction:

$$\begin{aligned} \mathcal{V}_c^{(4)}(r) &= -\frac{c\pi}{16}\frac{\delta^3(r)}{M_{4\mathrm{a}}} - \frac{c}{16M_{4\mathrm{b}}}\frac{\vec{P}^{\,2}}{r} - \frac{c}{32M_{4\mathrm{c}}}\left(\frac{\vec{P}^{\,2}-(\hat{r}\cdot\vec{P})^2}{r}\right) + \frac{3}{8}c\frac{r\vec{P}^{\,4}}{M_{4\mathrm{d}}}\cdot \\ &\quad + \left(\frac{c}{32r^3M_{\mathrm{LS1}}} + \frac{c}{8M_{\mathrm{LS2}}}\frac{\vec{P}^{\,2}}{r}\right)\vec{S}\cdot\vec{L} + \frac{c}{16r^3M^2m^2}Q_{12} \end{aligned} \tag{65}$$

Above the mass coefficients $M_{4\mathrm{j}}$ are defined as

$$M_{4\mathrm{a}} = \left(\frac{(M+m)^2}{M^3m^3} - \frac{1}{M^2m^2}\right)^{-1} \tag{66}$$

$$M_{4\mathrm{b}} = \left(\frac{3(M+m)^4}{M^4m^4} - \frac{8(M+m)^2}{M^3m^3}\right)^{-1} \tag{67}$$

$$M_{4\mathrm{c}} = \left(\frac{5(M+m)^4}{M^4m^4} - \frac{16(M+m)^2}{M^3m^3} + \frac{2}{M^2m^2}\right)^{-1} \tag{68}$$

$$M_{4\mathrm{d}} = \left(\frac{(M+m)^4}{M^4m^4} - \frac{3(M+m)^2}{M^3m^3} + \frac{1}{M^2m^2}\right)^{-1}, \tag{69}$$

and the mass coefficients for the spin-orbit interaction are defined as

$$M_{\mathrm{LS1}} = \left(\frac{1}{M^3}\left(\frac{3}{M}+\frac{2}{m}\right) + \frac{1}{m^3}\left(\frac{3}{m}+\frac{2}{M}\right)\right)^{-1} \tag{70}$$

$$M_{\mathrm{LS2}} = \left(\frac{1}{M^2m^2}\left(5 + \frac{3}{2}\left(\frac{M}{m}\right)^2 + \frac{3}{2}\left(\frac{m}{M}\right)^2\right)\right)^{-1}. \tag{71}$$

The structure of this term leads to the direct conclusion that one is dealing with an asymptotic series with little or no convergence or reliability, especially for the $\vec{P}$-dependent terms, since these show no sign of becoming progressively smaller. If one would try to continue this expansion to sixth order, one would already encounter terms that are either incalculable (e.g. $\nabla^6\frac{1}{r}$) or terms that have divergent matrix elements. However, since all these terms originate in well-behaved square root factors in the spinors, there is no doubt that in reality the velocity-dependence of the linear confining interaction is well-behaved. Therefore, some other treatment than the perturbative treatment of the expansion described above has to be used in the numerical analysis. In this work, a minimal form of the confining interaction is used, which takes into account only the central static part and the local spin-orbit and quadratic spin-orbit components from eqs. (63) and (65). This is admissible, since only the central and spin-orbit interactions are empirically motivated at this time. Please note that the remaining parts of eqs. (63) and (65) are included here for reference only.

The treatment of the nonlocal and nonstatic contributions to the confining interaction has often been unsatisfactory, partly because of the difficulties described above. A convenient way out of this difficulty is to assume that the confining interaction is not momentum dependent [16]. If however one wishes to examine the implications of scalar coupling for confinement in detail, one first has to find a method for converting the static, linear confining potential into a nonstatic form without excessive approximation. One possibility is to use eqs. (44) and (46) for this task, although it has already been noted that taking the limit $\lambda \to 0$ in eq. (46) analytically renders the inverse Fourier transform divergent. The trick is then to compute $V_c(r)$ as

$$V_c(r) = \lim_{\lambda \to 0} \int_0^\infty \frac{d^3k}{(2\pi)^3} e^{i\vec{k}\cdot\vec{r}}\, V_c(k,\lambda)\, f(k), \tag{72}$$

where it is understood that the limit is taken by performing the integration for smaller and smaller values of λ. $f(k)$ is a relativistic modification factor arising from eq. (47). Eq. (72) would thus yield a local potential in coordinate space. If the limit is taken numerically in the manner described above, $V_c(r)$ will be well-behaved as long as λ is nonzero. Furthermore, the resulting potential is numerically stable as $\lambda \to 0$. There are still huge difficulties in performing the integration in eq. (72) numerically for small enough values of λ. Ideally, one would like to have a potential that remains linear to at least 2 fm in the static limit before the effect of the exponential in eq. (44) starts to show. This corresponds to having $\lambda \leq 0.05\,\mathrm{fm}^{-1}$, which is already quite troublesome to integrate properly in momentum space. This problem becomes significantly worse if one would require 4 fm of linear potential instead of 2 fm. However, it is important to realize that relativistic modifications to the linear potential are important when $\vec{k}$ is large, which corresponds to small values of r. On the other hand, the "artificially" introduced exponential in eq. (44) will be noticeable only for large values of r, where the relativistic modifications will have little or no effect. Thus, when λ is sufficiently small, the exponential cutoff will not affect the range where the relativistic modifications are important. It then follows that the artificial cutoff can be removed **after** the integration, provided that $\lambda \leq 0.05$. Thus the proper way to proceed is to calculate the nonstatic form of the linear confining interaction by

$$\mathcal{V}_c(r) = e^{\lambda r} \int_0^\infty \frac{d^3k}{(2\pi)^3} e^{i\vec{k}\cdot\vec{r}}\, V_c(k,\lambda)\, \left(\frac{M+m}{e_Q + e_{\bar{q}}}\right), \tag{73}$$

which, provided that λ is small enough, gives the correct relativistic modification at small r as well as a linear potential at large r. Here the abbreviations $e_Q = \sqrt{M^2 + k^2/4}$ and $e_{\bar{q}} = \sqrt{m^2 + k^2/4}$ have been used. The other components of the confining interaction, e.g. spin-orbit can in principle be treated in exactly the same manner. If one notes that the scalar structure of the confining interaction implies functional relations between the different components of the potential, expressions for the confining spin-orbit interaction can be obtained. Thus e.g. in the static limit the spin-orbit component may be calculated from the central component as

$$V_{LS}(r) = -\frac{1}{4}\left(\frac{1}{M^2} + \frac{1}{m^2}\right)\frac{1}{r}\frac{\partial}{\partial r} V_c(r). \tag{74}$$

Here $V_c(r)$ is the central confining potential and $V_{LS}(r)$ is the coefficient function for the spin-orbit coupling operator $\vec{S}\cdot\vec{L}$. When the static limit is not invoked, the corresponding relation is more complicated. As for the central confining interaction, a nonstatic expression may be obtained as

$$\mathcal{V}_{LS}(r) = -\frac{1}{r}\frac{\partial}{\partial r}\int_0^\infty \frac{d^3k}{(2\pi)^3}\, e^{i\vec{k}\cdot\vec{r}} \frac{1}{2}\left(\frac{M+m}{e_Q + e_{\bar{q}}}\right)\left(\frac{1}{e_Q(e_Q+M)} + \frac{1}{e_{\bar{q}}(e_{\bar{q}}+m)}\right) V_c(\vec{k}), \tag{75}$$

which apparently suffers from the same convergence problems as the central interaction. However, in this case, one may actually set $\lambda = 0$ in $V_c(\vec{k})$ analytically, since the differentiation contributed by the spin-orbit operator renders the inverse Fourier transform convergent. The description of

the spin-orbit interaction also remains realistic as this limit is taken. Thus, a convenient nonstatic form for the confining spin-orbit interaction may be obtained as

$$\mathcal{V}_{LS}(r) = -\frac{2}{\pi}\frac{c}{r}\int_0^\infty dk \frac{j_1(kr)}{k}\left(\frac{M+m}{e_Q+e_{\bar{q}}}\right)\left(\frac{1}{e_Q(e_Q+M)}+\frac{1}{e_{\bar{q}}(e_{\bar{q}}+m)}\right). \tag{76}$$

It is thus evident that, even in the case of heavy quarkonia, the static expression for the confining spin-orbit interaction may be expected to represent a considerable overestimate of that effect. Further, it should be kept in mind that nonlocal effects may further decrease the effective spin-orbit contribution from the scalar confining interaction. Finally, the confining quadratic spin-orbit interaction may be treated in a similar way, although in that case the static expression is expected to be an even larger overestimate.

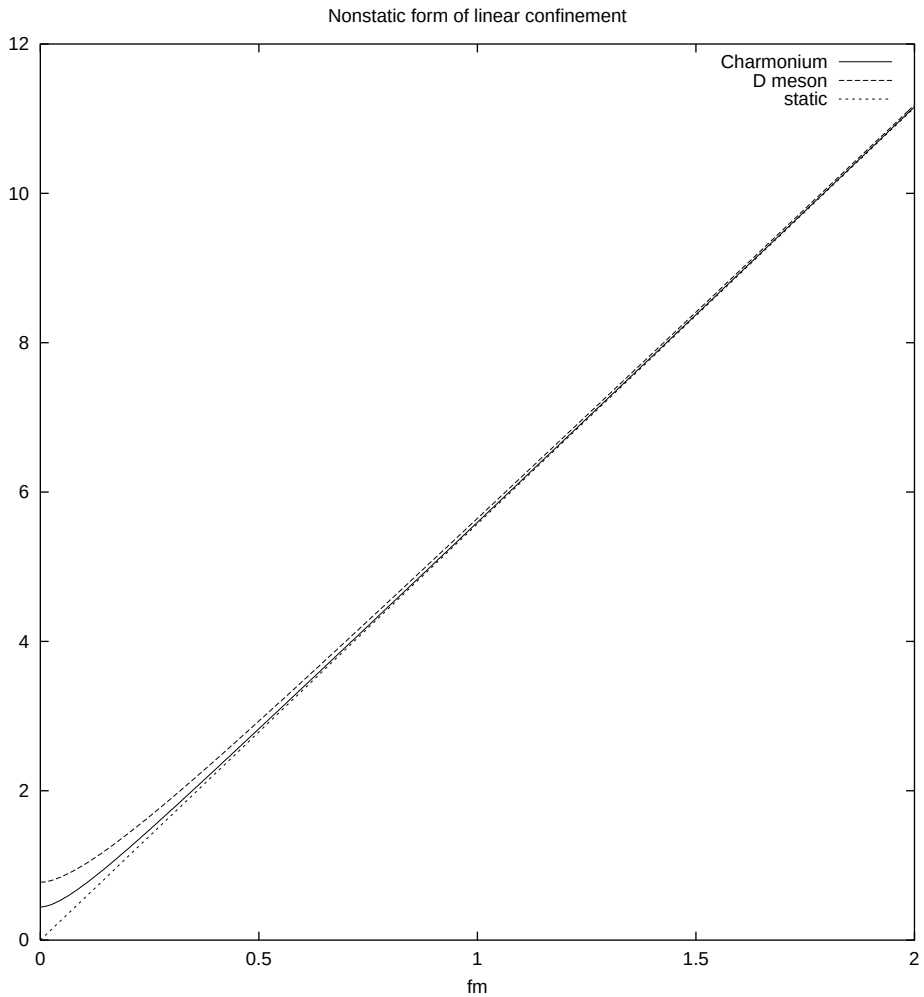

Figure 3: The effect of relativistic modifications to the linear confining interaction as calculated from eq. (73). The potentials correspond to $\lambda = 0.02\,\mathrm{fm}^{-1}$. The quark masses and the confining string constant are as given in Table 2.

So far, only the $\vec{k}$ dependent modifications to the confining interaction have been considered. A much more severe problem is the treatment of the nonlocal contributions to the scalar confining

interaction, i.e. the $\vec{P}$ dependent terms in eqs. (63) and (65). One possibility is to note that this effect may be viewed as a mass shift of the quarks up to second order in $\vec{P}$. This is readily seen by making the substitution

$$\frac{\vec{\nabla}^2}{2\mu} \longrightarrow \frac{\vec{\nabla}^2}{m^*} \tag{77}$$

in the BSLT equation. This amounts to taking the kinetic energy term from the BSLT equation and adding to this the nonlocal term from eq. (63). With the aid of the series expansion

$$\frac{1}{1+x} \approx 1 - x, \tag{78}$$

the expression for m^* is obtained as

$$m^* = 2\mu + \frac{3}{2} cr (\frac{2\mu}{m_2})^2. \tag{79}$$

This expression has the advantage of being more well-behaved than the quadratic form of eq. (63) but still has the same expansion to that order. This approximation is also compatible with the treatment of the confining interaction as a Lorentz scalar. This reveals that essentially, the nonlocal contribution amounts to a mass shift, increasing the effective quark masses with increasing distance. However, in this work, the nonlocal contribution to the scalar confining interaction has been treated in the following highly approximate fashion:

$$cr \left(1 - \frac{3}{2} \frac{\vec{P}^{\,2}}{{m_2}^2} \right) \approx cr + b. \tag{80}$$

In the above equation, if b is negative it may be viewed as an approximation of the nonlocal contribution to the confining interaction. This interpretation is new here, as most earlier work has treated b as a physical contribution to the confining interaction. Adding arbitrary constants to potentials has however no effect on the force nor the spin-orbit interaction between the constituent quarks, and thus it would be highly desirable to find an explanation for the origin of the constant b. Therefore, it seems natural to consider b as a contribution from the spinors and the BSLT factors, that vanishes for heavy quark masses. In this work, b takes on the values 170-350 MeV, being larger for lighter systems as expected. The calculations for charmonium indicate that this term should indeed be much smaller for heavy mesons. As this effect models the well-behaved velocity dependence in the Dirac spinors, it is also unlikely that the nonlocal contributions would be significantly stronger for the excited states. The approximation of this effect as a constant may therefore turn out to be plausible after all.

3.2 The one-gluon exchange interaction

In the case of heavy quarkonia the perturbative one-gluon exchange (OGE) interaction forms an important component of the hyperfine interaction between quarks. To second order in the inverse quark masses that interaction, as calculated from eq. (47), takes the following form in the BSLT formalism:

$$\begin{aligned}\mathcal{V}_g(r) &= -\frac{4}{3}\alpha_s\left\{\frac{1}{r}-\frac{3\pi}{2{m_2}^2}\delta^3(r)+\frac{\vec{P}^{\,2}}{2Mmr}\right\}\\ &+\frac{2\alpha_s}{3r^3}\left(\frac{M^2+m^2}{2M^2m^2}+\frac{2}{Mm}\right)\vec{S}\cdot\vec{L}-\frac{\alpha_s}{6r^3}\frac{M^2-m^2}{M^2m^2}(\vec{\sigma}_Q-\vec{\sigma}_{\bar{q}})\cdot\vec{L}.\\ &+\frac{8\pi}{9}\frac{\alpha_s}{Mm}\delta^3(r)\vec{\sigma}_Q\cdot\vec{\sigma}_{\bar{q}}+\frac{\alpha_s}{3Mmr^3}S_{12}+\frac{\alpha_s}{4r^5M^2m^2}Q_{12}.\end{aligned} \tag{81}$$

Note that in the Schrödinger formalism the numerical coefficients in the last two terms in the first bracket on the r.h.s. would be $-\pi$ and 1 instead of $-3\pi/2$ and $1/2$ respectively. Although this minimal form can be applied to heavy quarkonia with some success, this approach cannot be extended to account for the heavy-light mesons, as the constituent quarks in these systems are highly relativistic, which makes the expansion in the momentum transfer variable misleading. Fortunately, there is no need to make an expansion in $\vec{k}$, as this local variable can be directly integrated to produce a local potential $\mathcal{V}(r)$, that depends only on the quark-antiquark separation. The appropriate modification of the main term and accompanying delta function term in the one-gluon exchange interaction is thus:

$$-\frac{4}{3}\alpha_s\left\{\frac{1}{r}-\frac{3\pi}{2{m_2}^2}\delta^3(r)\right\}\rightarrow-\frac{4}{3}\frac{f_0(r)}{r}. \tag{82}$$

Here the function $f_0(r)$ is defined as

$$f_0(r)=\frac{2}{\pi}\int_0^\infty dk\frac{\sin(kr)}{k}\frac{M}{e_Q}\frac{m}{e_{\bar{q}}}\left(\frac{M+m}{e_Q+e_{\bar{q}}}\right)\alpha_s(k^2). \tag{83}$$

To reduce clutter, the factors e_Q and $e_{\bar{q}}$ are defined as

$$e_Q=\sqrt{M^2+\frac{k^2}{4}},\quad e_{\bar{q}}=\sqrt{m^2+\frac{k^2}{4}}. \tag{84}$$

This form gives the additional advantage of providing a means for direct incorporation of the effects of the running coupling of QCD into the central term of the OGE interaction. This important effect may be considered by making the replacement

$$\alpha_s\ \rightarrow\ \alpha_s(k^2). \tag{85}$$

For the running coupling of QCD, the following convenient parametrization [23] is used, where Λ_0 denotes the confinement scale and m_g the dynamical gluon mass, which functions as a cutoff at low momentum transfer:

$$\alpha_s(k^2)=\frac{12\pi}{27}\frac{1}{\ln[(k^2+4m_g^2)/\Lambda_0^2]}. \tag{86}$$

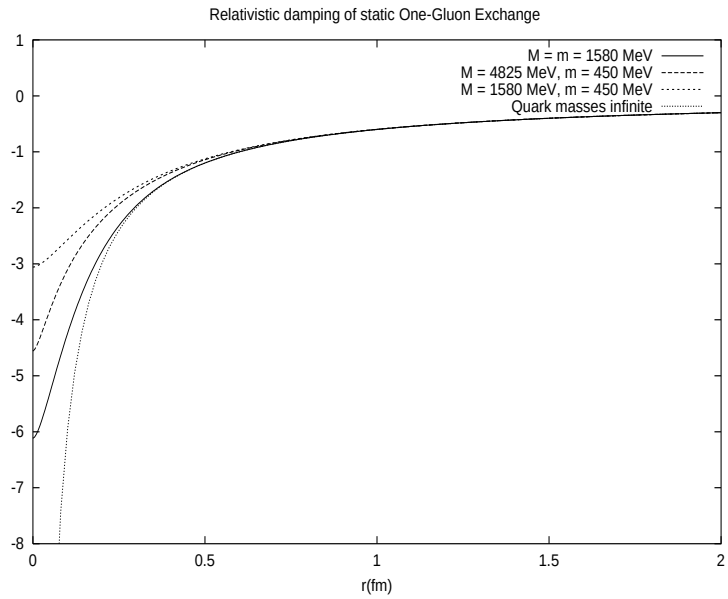

Figure 4: Illustration of the short-range relativistic dampening of the OGE interaction with constant coupling.

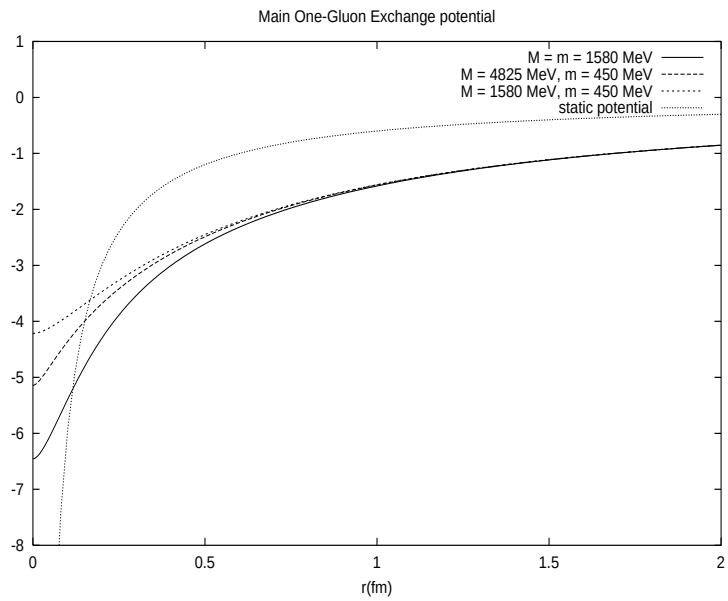

Figure 5: Comparison between the central component of the static OGE interaction with constant coupling and the form used here.

One of the most serious problems in quarkonium studies is the importance of the various nonlocal contributions to the main interaction. As these effects are non-negligible even for heavy quarkonia, they are certainly not less so for the heavy-light systems. Normally, the nonlocal contribution to the OGE interaction has been treated in first order perturbation theory only. However, the conclusion

here is that this treatment is seriously inadequate for the heavy-light systems, mainly for two reasons: Firstly, as the BSLT equation has an eigenvalue expression that differs radically from that in the Schrödinger equation, it is crucially important that the wavefunctions correspond to the spin-averaged energies of the various states. Otherwise, the relativistic dampening of the high-momentum part of the spectrum will lead to unrealistic results. Secondly, one has to keep in mind that if a running coupling for α_s is employed, there is little justification left to use perturbation theory at all. Therefore, in these calculation, the nonlocal term will enter the wavefunctions explicitly with no expansion in $\vec{k}$ to second order in $\vec{P}$. The expansion in $\vec{P}$ is still not satisfactory, but the abovementioned modifications make that term manageable for the present work. The appropriate modification of the $\vec{P}^{\,2}/r$ term in (81) is thus obtained by the replacement

$$-\frac{4}{3}\alpha_s\frac{\vec{P}^{\,2}}{2Mmr} \rightarrow -\frac{4}{3}\frac{f_2(r)}{r}\vec{P}^{\,2}, \tag{87}$$

where the function $f_2(r)$ is defined as

$$\begin{aligned} f_2(r) \;=\; & \frac{2}{\pi}\int_0^\infty dk\frac{\sin(kr)}{k}\left(\frac{e_Q+M}{2e_Q}\right)\left(\frac{e_{\bar{q}}+m}{2e_{\bar{q}}}\right)\left(\frac{M+m}{e_Q+e_{\bar{q}}}\right) \\ & \left\{\frac{4}{(e_Q+M)(e_{\bar{q}}+m)}-\frac{1}{2e_Qe_{\bar{q}}}+\frac{1}{(e_Q+M)^2}\left[1-\frac{M(e_Q+M)}{2e_Q^2}\right]\right. \\ & \left.+\frac{1}{(e_{\bar{q}}+m)^2}\left[1-\frac{m(e_{\bar{q}}+m)}{2e_{\bar{q}}^2}\right]\right\}\alpha_s(k^2). \end{aligned} \tag{88}$$

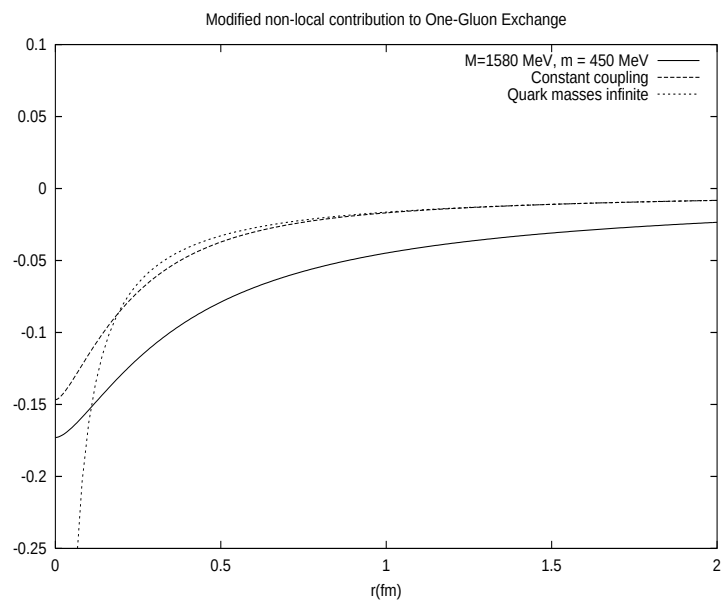

Figure 6: The $\vec{P}^{\,2}$ term for the OGE interaction. The case of constant coupling corresponds to α_s = 0.45.

Another serious problem in earlier work has been the correct inclusion of the spin-spin interaction into models of quarkonia. In the various static models this effect is always proportional to $\delta^3(r)$. This naturally leads to perturbative treatments, since this term cannot be included as such into any numerical calculations. However, this treatment usually gives much too large hyperfine splittings

for S-states and of course none at all for the higher orbital excitations. The unapproximated version of the spin-spin component of the OGE interaction is introduced by the replacement of the delta function as

$$\alpha_s \delta^3(r) \rightarrow \frac{1}{2\pi^2 r} \int_0^\infty dk k \sin(kr) \left(\frac{M+m}{e_Q + e_{\bar{q}}} \right) \frac{Mm}{e_Q e_{\bar{q}}} \alpha_s(k^2). \tag{89}$$

Although this form is moderated both by the running coupling of QCD and the BSLT square root factors, there still remains a singularity at zero quark separation. The general appearance is that of a smeared out delta function, which gives significant contributions also at longer range. The singularity at r=0 is no longer significant, since it is only logarithmic. This is less singular than 1/r, so the matrix element for S-states is finite numerically. In fact, there would be little difficulty in accounting for the spin-spin interaction explicitly, but in this case, it was decided that all hyperfine (spin-dependent) effects should be treated in first order perturbation theory. Since the wavefunctions now model the spin-averaged states, perturbation theory is expected to be somewhat more reliable in this case.

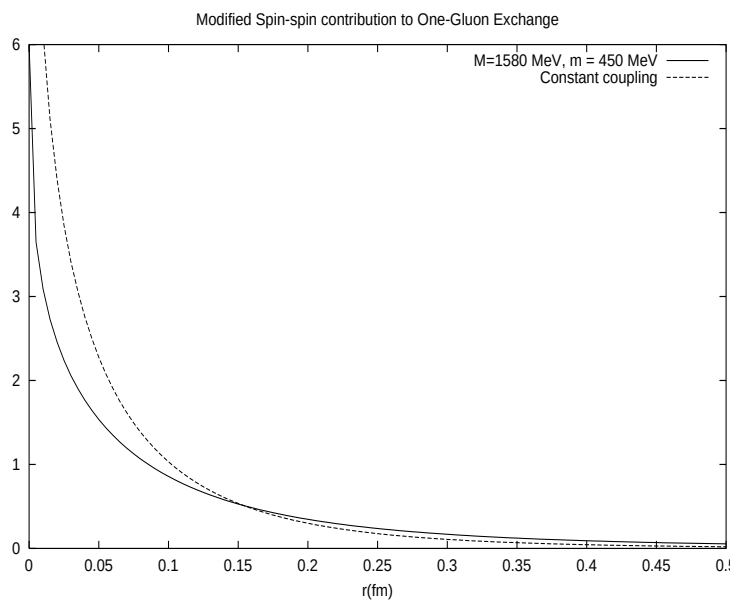

Figure 7: The unapproximated OGE spin-spin interaction, replacing $\alpha_s \delta^{(3)}(r)$. The case of constant coupling corresponds to $\alpha_s = 0.45$.

The present treatment of the spin-spin interaction has a few important ramifications: For phenomenological purposes, the delta function has sometimes been approximated as a smeared out Gaussian function, giving it some range as a consequence. One can now clearly draw the conclusion that this treatment is unrealistic, as the actual smeared-out form of the spin-spin interaction resembles an inverse logarithmic function, and is certainly not Gaussian at all. Secondly, especially for the charmed mesons (D and D_s) the P-states obtain a significant contribution of tens of MeV from the spin-spin interaction, which of course is absent in papers using the static form of the spin-spin interaction. The unapproximated form of the tensor interaction in (81) is obtained as

$$\mathcal{V}_G(T) = \frac{2}{9\pi} S_{12} \int_0^\infty dk k^2 j_2(kr) \left(\frac{M+m}{e_Q + e_{\bar{q}}} \right) \frac{\alpha_s(k^2)}{e_Q e_{\bar{q}}}, \tag{90}$$

and the corresponding modified form of the spin-orbit interaction as

$$\mathcal{V}_G(LS) = \frac{2}{3\pi r}\vec{S}\cdot\vec{L}\int_0^\infty dk\, kj_1(kr)\left(\frac{M+m}{e_Q+e_{\bar{q}}}\right)\left(\frac{e_Q+M}{e_Q}\right)\left(\frac{e_{\bar{q}}+m}{e_{\bar{q}}}\right)$$
$$\left\{\frac{1}{(e_{\bar{q}}+m)^2}\left[1-\frac{k^2}{4(e_Q+M)^2}\right]+\frac{1}{(e_Q+M)^2}\left[1-\frac{k^2}{4(e_{\bar{q}}+m)^2}\right]\right.$$
$$\left.+\frac{4}{(e_Q+M)(e_{\bar{q}}+m)}\right\}\alpha_s(k^2). \qquad (91)$$

Again, one of the more serious problems in quarkonia has always been the attempts to obtain realistic hyperfine splittings for the P-states. The need has been to balance and counteract the large spin-orbit splitting from the OGE interaction with that from the scalar confining interaction. This problem has been exacerbated by the disagreement on whether the confining interaction is a scalar or a vector in the spinorial structure, or some mixture of these. Further, there is the disagreement on the exact functional form of confinement. However, the fact that one easily gets gargantuan matrix elements for $\mathcal{V}_G(LS)$ is unavoidable if the standard static expressions are used. These can be somewhat moderated by using the nonstatic form of eq. (91). It also remains crucial to balance this term by the spin-orbit contribution from the scalar confining interaction. Thus the spin-orbit effects in quarkonia are conveniently explained by a scalar confining interaction, while a pure vector confining interaction only worsens the problem.

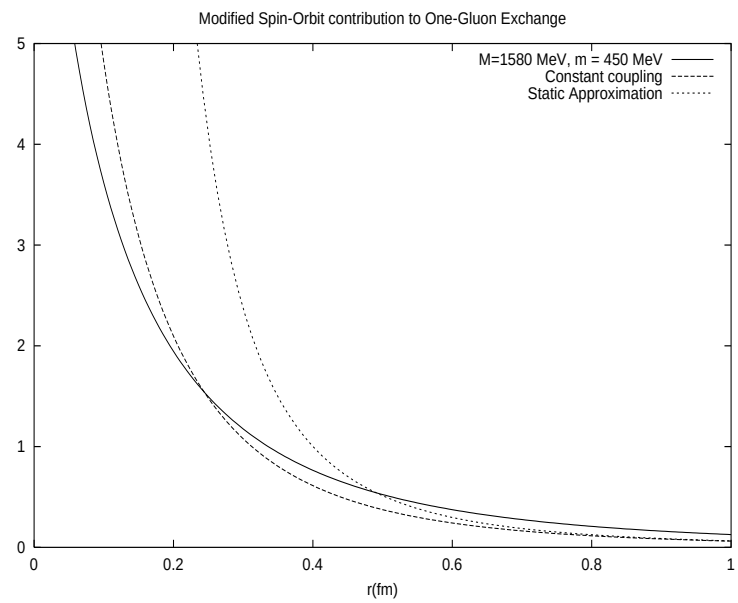

Figure 8: The unapproximated form of the OGE spin-orbit interaction $\mathcal{V}_G(LS)$. The case of constant coupling corresponds to $\alpha_s = 0.45$.

On the other hand, the tensor interaction component $\mathcal{V}_G(T)$ is found to be quite weak compared to the spin-orbit interaction. Nevertheless, this interaction is needed to reproduce the empirically observed splittings in charmonium and bottomonium, and therefore ought to be important for heavy-light systems as well, which indeed is found to be the case in the calculations for the bottom mesons. However, for charmed mesons the tensor interaction is insignificant in comparison to the dominant spin-orbit matrix element, which indicates that the spin-orbit interaction may be unrealistically large in these systems. The tensor interaction causes mixing between states with

different orbital angular momentum in second order perturbation theory. The weakness of the tensor interaction combined with the large level spacings in quarkonia makes this effect insignificant. However, the situation could still be quite the opposite for lighter systems like strangeonium ($s\bar{s}$), for which this argumentation is not necessarily applicable.

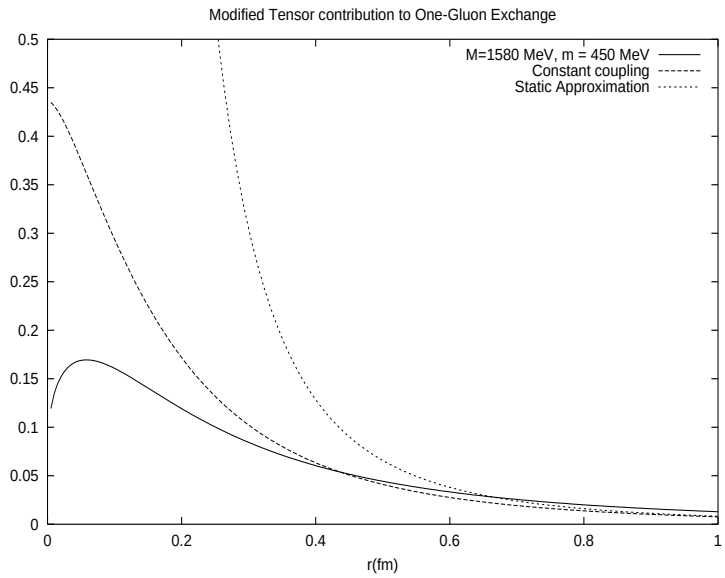

Figure 9: The unapproximated form of the OGE tensor interaction $\mathcal{V}_G(T)$. The case of constant coupling corresponds to $\alpha_s = 0.45$.

The quadratic spin-orbit interaction component, which is ill-behaved in the static limit, may be similarly regulated by employment of the unapproximated form:

$$\frac{\alpha_s}{4r^5M^2m^2} \to \frac{2}{3\pi r^2}\int_0^\infty dkk^2 j_2(kr)\frac{\alpha_s(k^2)}{e_Q e_{\bar{q}}(e_Q+M)(e_{\bar{q}}+m)}\left(\frac{M+m}{e_Q+e_{\bar{q}}}\right). \tag{92}$$

This form of the quadratic spin-orbit interaction has finite matrix elements. Usually the quadratic spin-orbit interaction has not been included in quarkonium studies, as it is of quartic order, and no doubt also because it is incalculable in the static limit for P-states, where it has nonvanishing matrix elements.

The parametrization (86) takes the long distance screening of the quark-gluon coupling into account through the gluon mass parameter m_g. The value $m_g = 240$ MeV has been chosen for the dynamical gluon mass, while for the confinement scale Λ_0, the value 280 MeV has been used. These values are not taken from any previous work, but are rather chosen by a fit to the heavy-light meson spectra. However, it has been endeavored to keep them similar to those implied by refs. [22, 23] to the extent possible. The employment of the relativistic modifications discussed in this section leads to significant dampening of the OGE interaction at short range, while the screened running quark-gluon coupling strength tends to have an opposite effect, mainly increasing the effective range of the interaction. The results reveal that the approximation $f_0(r) = \alpha_s =$ constant is inadequate. The parametrization (86) gives the value ≈ 0.4 for α_s at the charmonium scale and ≈ 0.25 at the bottomonium scale which is consistent with the values extracted by lattice methods in ref. [22]. It is thus concluded that in order to obtain realistic numerical results for the spectra of the heavy-light mesons, it is essential to use the unapproximated expressions for the functions $f_0(r)$ and $f_2(r)$, the reason being that the small mass of the light quarks render the static approximations misleading.

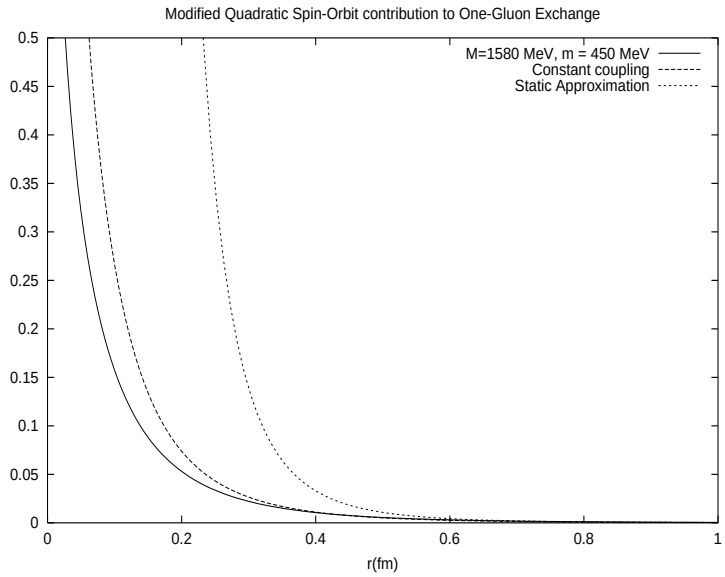

Figure 10: The unapproximated form of the OGE Quadratic spin-orbit interaction. The case of constant coupling corresponds to $\alpha_s = 0.45$.

3.3 The instanton induced interaction

Recent numerical lattice QCD calculations [24] provide strong evidence for important contributions to light hadron structure by instantons. The possible role of instantons in contributing to the structure of the heavy-light mesons has been investigated in [26] and [27]. For the heavy-light mesons, there exists both a spin-independent and a spin-dependent contribution from the instanton induced interaction. The spin-dependent part, that is given as [27]

$$H_{Q\bar{q}}^{\mathrm{Spin}} = -\frac{1}{4}\left(\frac{\Delta M_Q^{\mathrm{Spin}} \Delta m_{\bar{q}}}{2nN_C}\right) \vec{\sigma}_{\bar{q}} \cdot \vec{\sigma}_Q \, \lambda_{\bar{q}} \cdot \lambda_Q \, \delta^3(r), \tag{93}$$

couples as a T invariant $\sigma^1_{\mu\nu}\sigma^2_{\mu\nu}/2$, which implies that it may be viewed as a vector meson exchange like interaction with anomalous couplings to quarks. In [26, 27] the large N_C limit is considered, giving $\lambda_{\bar{q}} \cdot \lambda_Q/4 = -N_C/2$. Especially in that limit, the interaction (93) plays a role akin to that of the OGE interaction in splitting the heavy-light meson ground states, with matrix elements of similar magnitude [27]. The spin-spin interaction is determined to be about 80 MeV in the charmed mesons, which is about 60 % of the experimentally determined value, assuming no OGE interaction. However, the results obtained in ref. [27] must be regarded as rudimentary order-of-magnitude estimates only, since that model uses a slightly oversimplifying harmonic oscillator ansatz to provide a mechanism of confinement. In addition, the instanton induced interaction also contains a scalar part [26], giving for the spin-independent interaction

$$H_{Q\bar{q}} = \left(\frac{\Delta M_Q \Delta m_{\bar{q}}}{2nN_C}\right)\left(1 + \frac{1}{4}\lambda_{\bar{q}} \cdot \lambda_Q\right)\delta^3(r). \tag{94}$$

As can be seen, the scalar term vanishes in the large N_C limit, while the second "Coulomb-like" term remains and becomes attractive, which is a desirable feature. In the expressions (93)

and (94) n represents the instanton density, which is typically assigned the value 1 fm^{-4} [25]. ΔM_Q denotes the mass shift of the heavy quark, which renormalizes the strength of the instanton induced interaction and is generally concluded [25, 27] to be of the order 100 MeV. In the instanton models, the light quarks (u,d) are usually taken to be massless. $\Delta M_{\bar{q}}$ then denotes the mass shift (constituent quark mass) of the light quarks, and is taken in ref. [27] to be $\sim$ 420 MeV. The parameter $\Delta M_Q^{\mathrm{Spin}}$, which controls the strength of the spin-spin interaction is given in [27] as 3 MeV in the case of a charm quark.

Since it appears to be possible to produce spectra with sufficient spin-spin splitting using the OGE interaction alone, the calculations do not include the instanton induced interaction. In ref. [25] it is noted that the instanton induced interaction has the desirable feature of enabling one to avoid using an unrealistically large value for the strong coupling α_s. Since a constant value for α_s is not used here, this argument does not apply to the present work. Still, the extra attraction provided by eq. (94) would be a desirable feature for the heavy-light meson spectra. One may further speculate that a completely relativistic treatment of the OGE spin-spin interaction including all the nonlocalities may render it too weak to account for e.g. all of the observed $D^* - D$ splitting, thus leaving room for the instantons as well.

Finally it is worth noting that attempts have been made for quite some time now to account for confinement through the instanton induced interaction. Ref. [25] presents a thorough historical discussion on this topic, which illustrates the large variety of ways in which instantons could be made to account for confinement. The most common propositions include objects with fractional topological charge, strongly correlated instantons and the effects of very large instantons. In ref. [11] it is shown that the radial potential generated by an instanton ensemble, which can also be derived analytically, leads to a quadratically rising potential at small r which becomes approximately linear at intermediate ranges. However, this potential is known to flatten out at large r and asymptotically approach a constant value, which is related to the renormalization of the heavy quark mass ΔM_Q. It is therefore generally assumed that the instantons do not confine, at least not by means of an infinitely rising potential. However, [11] also speculates on how instantons could cause confinement even in the absence of an infinitely rising potential. For instance, since chiral symmetry breaking gives the light quarks a constituent mass, it may be energetically favorable to produce one or several pions instead of a light quark-antiquark pair. Further, [11] derives a condition under which the heavy quarks become unstable under decay to B or D mesons.

It seems at this time that the role of instantons for the lighter hadrons (and possibly the heavy ones as well) is well established at a qualitative level. What would be desirable now is to obtain quantitative field theoretical interaction models, which could be used in calculations to the same degree of accuracy as OGE and OPE. The heavy-light mesons would be interesting objects to study here, since they represent systems that are likely to share features encountered in both heavy and light quark physics. The source of the observed heavy-light meson structure will probably turn out to be a mixture of the confining, OGE and instanton induced interactions. This is even more probable if one notes that the large relativistic dampening of the OGE interaction for light quarks effectively precludes it from playing a dominant role in the case of light hadrons.

4 Solution of the Schrödinger-type equation

4.1 Numerical methods

Having established the interaction potentials to be used, the remaining task is to solve the BSLT equation numerically in order to obtain spectra and wavefunctions. It is here that the similarity of the BSLT equation and the Schrödinger equation becomes most useful. The problem then reduces to the standard problem of finding the solutions to a second-order eigenvalue equation, for which there exists a number of well-established numerical algorithms. In this work the Runge-Kutta-Nyström (RKN) algorithm [38] is used. The RKN is an integration algorithm for an arbitrary second-order differential equation which requires boundary values at the starting point, which in this case is naturally chosen as r=0. Expressions for the solution itself and its derivative are therefore required at the origin.

In fact, this would already be sufficient to obtain the entire wavefunction, by demanding that the solution behave correctly asymptotically. However, in order to increase accuracy and to clarify the computations, it is convenient to start the RKN algorithm also at large r, in this case $r = 4$ fm. An arbitrary intermediate point is thereafter chosen, for example r=0.5 fm, where the two solutions are compared. The outer solution is multiplied by a suitable factor to make the wavefunction continuous at this point. The correct energy eigenvalue (ϵ) can then be found by demanding that the derivative of the wavefunction at $r = 0.5$ fm also be continuous. In principle, this procedure makes it possible to determine the eigenvalues for a given set of potential parameters (masses, coupling constants) with an accuracy of at least 0.01 MeV. The principal quantum number of the obtained solution is identified by the number of oscillations. The ground state wavefunction does not change sign, the first excited state oscillates once and so on. In practice, the state energies are found by "guessing" a value for E, from which ϵ is then computed and inserted into the differential equation. Thereafter, the "guess" is improved until the derivatives at r=0.5 fm are indistinguishable. In this way the reduced wavefunctions $u(r)$, which are defined as

$$\psi_{\mathrm{nlm}}(\vec{r}) = \frac{u_{\mathrm{nl}}(r)}{r} Y_{\mathrm{lm}}(\Omega), \tag{95}$$

are obtained. Here Y_{lm} denotes the angular part of the solution, the spherical harmonics [39], which can always be determined analytically since all the interaction potentials are radially symmetric and thus depend only on r. The spherical coordinates are used throughout the computations. Thus the equation to be solved numerically reads [40]

$$\left(-\frac{1}{2\mu} \frac{\mathrm{d}^2}{\mathrm{d}r^2} + \frac{l(l+1)}{2\mu r^2} + \mathcal{V}(r, \vec{P}^{\,2}) \right) u(r) = \epsilon u(r), \tag{96}$$

where the ansatz (95) has been applied. In the above expression, the centrifugal barrier, arising from the angular part of ∇^2 operating on the spherical harmonics, is given explicitly. The interaction potential $\mathcal{V}$ now consists of various local contributions, and nonlocal contributions up to order $\vec{P}^{\,2}$ can be included explicitly, provided that they do not overwhelm the first term on the left-hand side in (96), by the following substitution,

$$\frac{1}{2\mu} \longrightarrow \frac{1 - \frac{8\mu}{3} \frac{f_2(r)}{r}}{2\mu} \tag{97}$$

where the expression for the nonlocal contribution to the OGE interaction has been inserted. In this context it is worth noting that if the numerator in eq. (97) becomes zero, the RKN algorithm becomes ill-behaved. In the static limit (81) this is the case. When the unapproximated form of eq. (88) is used instead, this problem disappears. It may thus be conjectured that if one would treat the confining interaction in an equivalent unapproximated way, the velocity dependence of that interaction would also be more well-behaved. For the Schrödinger type equation, the solution near r=0 always behaves as [40]

$$u(r) = r^{l+1} + Br^{l+2} + Dr^{l+3} + \dots \ , \tag{98}$$

where l denotes the orbital angular momentum quantum number. When the BSLT equation is considered, the coefficient B vanishes since there are no $1/r$ contributions to the potential. By taking the coefficient D into account, $u(r)$ may be expressed as

$$u(r) = r^{l+1} \left\{ 1 - \frac{\mu}{2l+3} \left(\epsilon - b + \frac{4}{3} \frac{f_0(r)}{r} \right) r^2 \right\}, \tag{99}$$

where it is understood that μ has been modified according to eq. (97). The constant b that appears here is discussed in section 3.1. By expanding the solution for large r, one can similarly obtain an expression for the asymptotic behavior of the solution, which follows directly from a linear potential at large r:

$$u(r) \propto e^{-ar^{\frac{3}{2}}}, \tag{100}$$

where the constant a is given as

$$a = \frac{2}{3}\sqrt{2\mu c}. \tag{101}$$

Here, the proper expressions for the wavefunction boundary values have been worked out in detail. However, it actually turns out that the solutions are extremely insensitive to the exact form of the boundary values, as errors soon cancel out provided that the RKN-routine itself contains the correct information about the potential used. This suggests that one could in fact drop out the second term in (99) entirely and still obtain quite accurate energy eigenvalues. However, since the current model contains various extremely short-ranged contributions that are consequently very sensitive to the exact form of the wavefunction near the origin, it was decided not to approximate the solution in this manner.

4.2 Integration of potentials

The static quark model is not used in this work. Put in another way, $\vec{k}$ is not assumed to be small. This leads to a situation where the potentials are no longer simple analytic functions of r, but are rather given as r-dependent integrals over $\vec{k}$-space. These expressions, which replace the standard static ones in eq. (81) can be found in section 3.2. As there is no expansion in $\vec{k}$, there will be less terms in the unapproximated version of eq. (81). For example, no Darwin-Foldy terms will appear. The RKN algorithm requires input values of $\mathcal{V}(r)$ preferably obtainable at arbitrary r. For this purpose, functions in Fortran 90 have been constructed that require as input the parameters governing $\alpha_s(k^2)$ and the value of r in fermi units. These functions then perform the integration over $\vec{k}$ for the chosen value of r. The integration ranges and number of data points used for each function are listed in Table 1.

Potential	k_{max}	Number of points
$f_0(r)$	300	4000
$f_2(r)$	300	4000
$\alpha_s\delta^3(r)$	20000	20000
$\mathcal{V}_G(LS)$	2000	5000
$\mathcal{V}_G(T)$	20000	20000
$\mathcal{V}_G(Q)$	20000	20000

Table 1: Integration ranges and number of points in the Simpson algorithm [38] used to obtain nonstatic expressions for the OGE interaction.

It is worth noting here that the hyperfine interaction contributions require a large number of data points and long integration ranges compared to the leading ones. This is because the hyperfine contributions are more singular in the static approximation, and consequently the nonstatic forms must be more ill-behaved. In the case of the spin-spin deltafunction in Table 1 there exists a logarithmic singularity at $r = 0$. The form implemented here ensures that the integral converges for $r = 0.05$ fm, which is the smallest r-value that enters the RKN algorithm explicitly. The general behavior of the integrands in k-space is the following: If r is small, the integrand is dominated by the k-dependence of the potential itself, and tends to converge rather slowly, thus requiring long integration range to cover the entire integrand. For $r \leq 1$, the spherical Bessel functions dominate, leading to rather short-ranged but rapidly oscillating integrands. In order to pick up all oscillations, the number of points in the Simpson routine must be large. Consequently, both densely spaced points and long integration ranges are required if one wishes to obtain accurate results for all values of r.

4.3 Wavefunctions

In the current model, all spin-independent effects considered are included explicitly into the RKN-routine, and thus the wavefunctions model the spin-averaged states of the systems considered. In the following sections, these contributions will be denoted by H_0, which is given as

$$H_0 = -\frac{\nabla^2}{2\mu} + \mathcal{V}(r, \vec{P}^{\,2}), \tag{102}$$

where the leading terms from the confining and OGE interactions have been included, in addition to the nonlocal contribution from the OGE interaction. The constant b, which is discussed in section 3.1 is also included. Thus $\mathcal{V}(r, \vec{P}^{\,2})$ is given as

$$\mathcal{V}(r, \vec{P}^{\,2}) = cr + b - \frac{4}{3}\frac{f_0(r)}{r} - \frac{4}{3}\frac{f_2(r)}{r}\vec{P}^{\,2}. \tag{103}$$

The various other contributions will be considered in first order perturbation theory, and can be expressed in the following form:

$$H_{\rm HYP} = H_{\rm SS} + H_{\rm SO} + H_{\rm T} + H_{\rm Q}. \tag{104}$$

Here $H_{\rm SS}$ contains the spin-spin interaction from OGE (eq. 89), while $H_{\rm SO}$ contains the local spin-orbit contributions from both OGE and confinement (eqs. (91), (63) and (65)). $H_{\rm T}$ contains the tensor (S_{12}) interaction from OGE (eq. 90), and finally $H_{\rm Q}$ contains the quadratic spin-orbit components from eqs. (92) and (65). The contribution from the hyperfine interaction components is obtained numerically in first order perturbation theory by performing the integration

$$\int_0^\infty d^3r\, \psi^*(\vec{r}) H_{\rm HYP}\, \psi(\vec{r}). \tag{105}$$

For this purpose, numerical expressions for the expectation values of the various interaction operators that appear in the potential are needed for different total angular momentum J, total orbital angular momentum L and total spin S quantum numbers. These may be obtained from the following formulae, see for example ref. [10]:

$$\langle \vec{\sigma}_Q \cdot \vec{\sigma}_{\bar{q}} \rangle = 2s(s+1) - 3, \tag{106}$$

$$\left\langle \vec{S} \cdot \vec{L} \right\rangle = \frac{1}{2}\left(j(j+1) - l(l+1) - s(s+1)\right), \tag{107}$$

$$\langle S_{12} \rangle = -2\left(\frac{6\left\langle \vec{S} \cdot \vec{L} \right\rangle^2 + 3\left\langle \vec{S} \cdot \vec{L} \right\rangle - 2s(s+1)l(l+1)}{(2l-1)(2l+3)} \right). \tag{108}$$

In this work the quadratic spin-orbit interaction, which contributes to the orbitally excited states, is considered as well. The matrix elements of the quadratic spin-orbit interaction operator Q_{12} can be expressed in the following form:

$$\langle Q_{12} \rangle = \begin{cases} -l(l+1) & \text{if } S = 0, \\ \begin{cases} j = l & \to\ 1 - l(l+1) \\ j = l+1 & \to\ l^2 \\ j = l-1 & \to\ (l+1)^2 \end{cases} & \text{if } S = 1. \end{cases} \tag{109}$$

Note that the quadratic spin-orbit interaction does not contribute at all when $L = 0$. The general features of the quarkonium wavefunctions are briefly discussed. The main emphasis is on the D-meson, since the wavefunctions of the other heavy-light mesons are qualitatively similar.

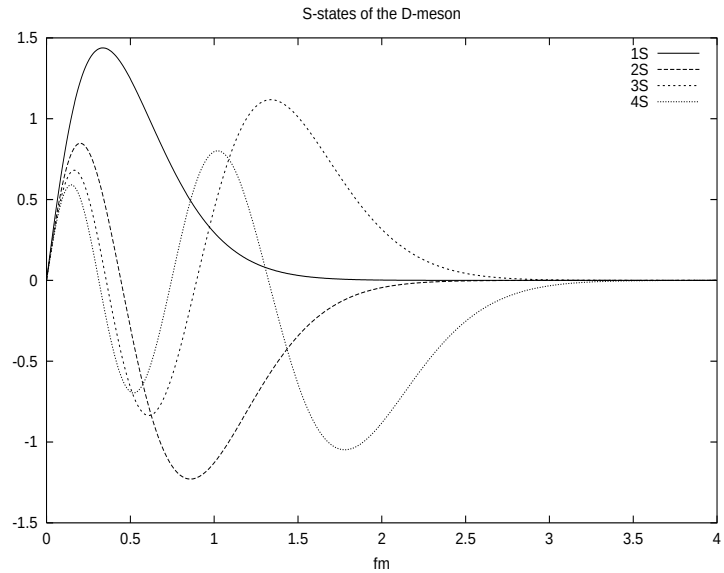

Figure 11: Reduced wavefunctions $u(r)$ for the first four states of the D-meson with zero orbital angular momentum, corresponding to the parameters in Table 2.

It is apparent from Fig. 11 that the D-wavefunctions are very narrow, the root-mean-square radius being less than 0.5 fm for the ground state. This narrowness is of extreme importance since it allows for matrix elements of the spin-spin interaction that are compatible with experimental data. Here it is worth noting that if the nonlocal term from OGE were not to be included explicitly in the wavefunctions, agreement with the empirical data for the spin-spin splittings would be excluded for the charmed mesons. If one would then attempt to compensate with the additional spin-spin dependence from the instanton induced interaction, one would end up with much too large splittings for the bottom mesons. In the case of the radial excitations of the D-meson, the states with $l = 1$ and $l = 2$ have been included, since these are all likely to be discovered in the near future. It is instructive to compare the S-, P- and D-state wavefunctions in Fig. 12, since these show the effect of an increasing centrifugal barrier by pushing the wavefunction away from the origin. Thus spin-spin interactions are expected to be small for states with nonzero l. For heavy quarkonia, this is indeed a plausible argument, but since the modified spin-spin interaction here has nonzero range, the charmed mesons obtain a significant contribution of order 30 MeV from this interaction.

Finally, a comparison between mesons with one charm quark, and a $\bar{c}$, $\bar{s}$ or $\bar{u}$ antiquark is presented in Fig. 13. In this case the wavefunctions will be broader for the lower mass mesons, because of the increased repulsion associated with the kinetic energy, although this repulsion is now strongly moderated because of the relativistic treatment of the kinetic energy, and is no longer a dominant effect as in the nonrelativistic Schrödinger equation.

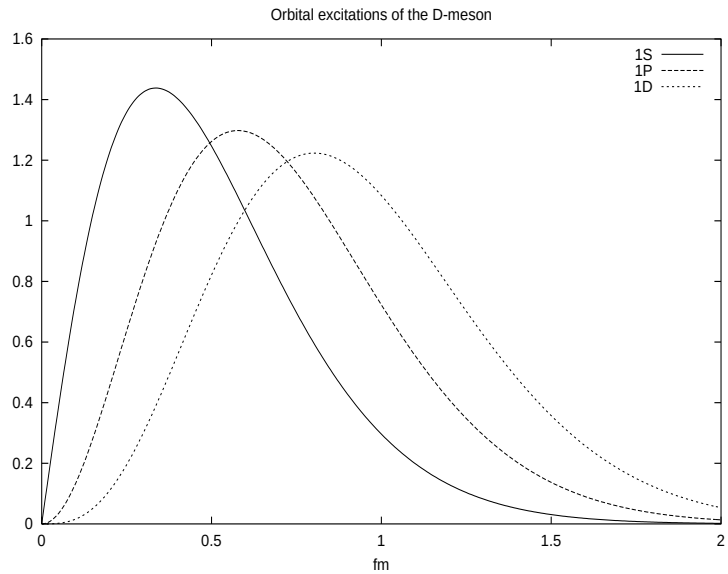

Figure 12: Reduced wavefunctions $u(r)$ for the 1S, 1P and 1D states of the D-meson, corresponding to the parameters in Table 2.

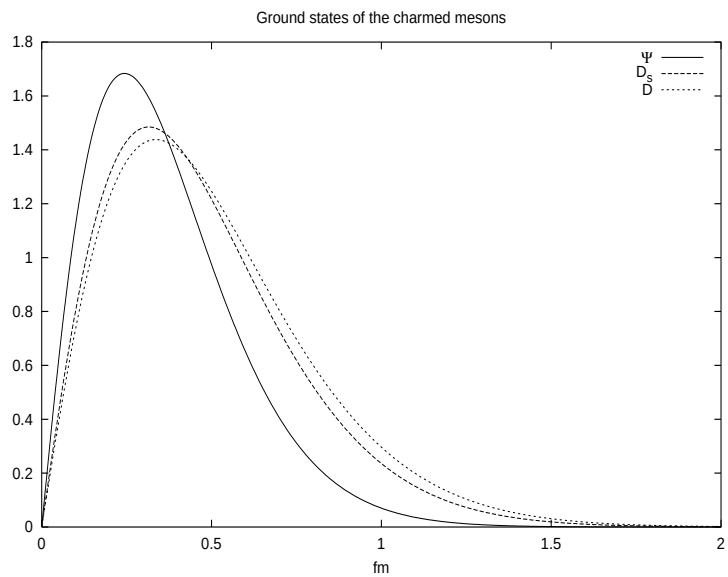

Figure 13: Comparison between the $c\bar{c}$, $c\bar{s}$ and $c\bar{u}$ ground states, for the parameters in Table 2.

5 The spectra of charmonium and the heavy-light mesons

5.1 General Considerations

The interaction model used for obtaining the spectra of the heavy-light mesons consists of all the contributions to the Hamiltonian given in Section 4.3, with full account of the relativistic corrections and the running coupling strength as described in Section 3.2. In obtaining a fit to the empirical heavy-light meson spectra, the value of the string constant c for the scalar confining interaction was chosen to be similar to that used in [10]. The parameter Λ_0 was kept in reasonable agreement with the results obtained by lattice QCD calculations for the bottomonium and charmonium scales in [22]. On the other hand, m_g is treated as a phenomenological parameter to be determined by a fit to the meson spectra. The heavy quark masses are to some extent treated as free parameters, with the restriction that they should be in the range 1400-1600 MeV for the c quark and 4600-4900 MeV for the b quark. The light quark masses are treated as phenomenological parameters to be fitted against the known splittings in the heavy-light meson spectra. The parameter b is treated phenomenologically, with the restriction that it must increase in magnitude for the lighter mesons, so as to model the nonlocal contribution from the confining interaction.

When computations were performed, the D-meson spectrum was taken as a starting point, yielding a value for the c and u,d quark masses. Thereafter the spectrum of the D_s meson was calculated without modification of the charm quark mass, thus yielding a value for the mass of the strange quark. Then the obtained parameters were tested by direct computation of the $c\bar{c}$ spectrum, without further modification of the charm quark mass.

	$c\bar{c}$	D_s	D
c	1120 MeV/fm	1120 MeV/fm	1120 MeV/fm
b	-50 MeV	-260 MeV	-320 MeV
Λ_0	280 MeV	280 MeV	280 MeV
m_g	240 MeV	240 MeV	240 MeV
m_c	1580 MeV	1580 MeV	1580 MeV
m_s	-	560 MeV	-
$m_{u,d}$	-	-	450 MeV

Table 2: Model parameters used for the charmonium, D and D_s meson spectra.

With the parameter values listed in Table 2 it is possible to accurately reproduce the experimentally determined J/Ψ-η_c splitting, but at the price of 30-50 MeV overpredictions of the excited states. This effect is similar to that noted in [15][1]. Better agreement with experiment can be achieved by lowering the confining string constant to 960 MeV/fm and raising the gluon mass m_g by 20 MeV to 260 MeV. In that case the excited states agree fairly well with experiment, while the J/Ψ-η_c splitting is underpredicted by 15 MeV. A lower charm quark mass for the charmonium system would also improve the spectra, but as the charmonium spectrum is calculated primarily for testing purposes, the charm quark mass is kept equal to that used for the D and D_s-mesons. The quality of the spectrum is similar to that obtained with an effective interaction constructed by means of lattice methods [10], as well as by completely nonrelativistic phenomenology [1, 17]. The numerical values for the calculated energies of the $c\bar{c}$ are listed in Table 3, along with the experimental values [30] and those obtained in ref. [15].

[1]Note that this reference quotes the calculated states to the nearest 10 MeV.

	Predicted	ref.[15]	Experimental
1^1S_0	2975	3000	2979.8 ± 2.1
1^3S_1	3088	3100	3096.88 ± 0.04
2^1S_0	3682	3670	
2^3S_1	3736	3730	3686.00 ± 0.09
1^1P_1	3518	3510	
1^3P_0	3450	3440	3417.3 ± 2.8
1^3P_1	3519	3500	3510.53 ± 0.12
1^3P_2	3580	3540	3556.17 ± 0.13

Table 3: Calculated and experimental energies of the most important charmonium ($c\bar{c}$) states. The calculated energies are compared to ref.[15]. All energies are given in MeV.

The value of the b quark mass is obtained by a fit to the B-meson spectra, after which all parameters in the model are determined. Thus the only adjustable parameter left in the calculation of the B_s spectrum is b. This also provides a consistency check for this parameter. Throughout the calculations, Λ_0, m_g and c have been forced to remain constant. Likewise the quark masses are not allowed to vary. These, in some sense trivial (apart from c) constraints nonetheless demand much of the realism of the model used, since it has been simultaneously applied to four different systems.

	B_s	B
c	1120 MeV/fm	1120 MeV/fm
b	-185 MeV	-250 MeV
Λ_0	280 MeV	280 MeV
m_g	240 MeV	240 MeV
m_b	4825 MeV	4825 MeV
m_s	560 MeV	-
$m_{u,d}$	-	450 MeV

Table 4: Parameter values used in the calculation of the B_s and B-meson spectra.

The next sections contain a detailed analysis and presentation of the obtained results for the heavy-light mesons considered.

5.2 The D and D_s -meson spectra

As mentioned earlier, in the calculation of the spectra of the D and D_s mesons, the constituent masses of the light and strange quarks are treated as phenomenological parameters to be fitted against the known splittings in the spectrum. This is so because of the relativistic nature of the light quark in these systems. If the nonlocal $\vec{P}^2$ contribution were treated exactly, more physical significance could be attached to the obtained light quark masses. These are here about 100 MeV larger than the typical values employed in nonrelativistic phenomenology. Reducing these masses further in the calculation would lead to an unrealistically large spin-orbit splitting of the $P-$ states, while giving an unrealistically small 1S $\rightarrow$ 2S spacing. Thus the main reason for using somewhat higher constituent quark masses is the need to counteract the nonlocal contribution from the OGE interaction. Consequently some accuracy in the spectra had to be sacrificed in order to obtain constituent quark masses that can be expected to be realistic in calculations of M1 transitions. It may be conjectured that treating the nonlocalities exactly may raise the D meson ground state by ~ 30 MeV and the first excited state by as much as 150 MeV. In this case one might obtain good spectra with even lower constituent quark masses.

	ϵ	H_0	$H_0 + H_{\rm HYP}$	Ref. [15]	Exp(D^0)	Exp($D^\pm$)	$\sqrt{\langle r^2 \rangle}$
1^1S_0	-0.28	1973	1874	1850	1864.6±0.5	1869.3±0.5	0.48
1^3S_1			2006	2020	2006.7±0.5	2010.0±0.5	
2^1S_0	3.76	2586	2540	2500			0.90
2^3S_1			2601	2620	2637 ?	2637 ?	
3^1S_0	6.93	2936	2904	2980			1.27
3^3S_1			2947	3070			
4^1S_0	9.68	3200	3175	3370			1.60
4^3S_1			3208				
1^1P_1	2.50	2427	2389	2410			0.70
1^3P_0			2341	2270			
1^3P_1			2407	2400	2422.2±1.8		
1^3P_2			2477	2460	2458.9±2.0	2459 ± 4	
2^1P_1	5.82	2820	2792				1.10
2^3P_0			2758	2780			
2^3P_1			2802	2890			
2^3P_2			2860	2940			
3^1P_1	8.66	3105	3082	3300			1.45
3^3P_0			3050	3200			
3^3P_1			3085	3290			
3^3P_2			3142	3340			
1^1D_2	4.79	2708	2689	2760			0.91
1^3D_1			2750				
1^3D_2			2727				
1^3D_3			2688				
2^1D_2	7.71	3014	2997	3170			1.29
2^3D_1			3052				
2^3D_2			3029				
2^3D_3			2999				

Table 5: Calculated and experimental D meson states. The first column gives the ϵ values for the spin-averaged states, and the second column gives the corresponding state energies. The third column gives the results for the complete Hamiltonian. These data are compared to ref. [15] and to experimental data when available. All energies are given in MeV. The rightmost column lists the computed rms radii of the different states in fm units.

The calculated energies of the D meson states are listed in Table 5 along with the known empirical energies [30]. The calculated D meson spectrum has about the correct $D^* - D$ ground state splitting, underpredicted by only 10 MeV. The model used here only slightly underpredicts the possible D meson excitation [31, 32] at 2637 MeV. In addition, the P-shell states around 2400 MeV are also satisfactorily reproduced. It is worth noting that the current model differs from [15] and indeed from all earlier models by the significantly smaller spin-spin splittings of the excited states, as is evident from Table 5. Apparently this is a consequence of both the relativistic dampening of the spin-spin interaction and the disappearance of the Coulombic singularity in the main OGE potential. Whether this feature is supported by experimental data still remains to be seen. At this time only in the $c\bar{c}$ system has a candidate for an excited $l = 0$ singlet state been seen, but even this is nowadays considered doubtful. Since even in charmonium, singlet states cannot be produced in e^+e^- collisions, their detection may remain a formidable task in the near future. The main difficulty with the spin-orbit splittings may be ascribed to the small mass of the light quarks, which makes the matrix elements of the spin-orbit components of both the confining and hyperfine interactions large. Further, because there is destructive interference between the

OGE and confining spin-orbit interactions, this problem is exacerbated. The spin-orbit splitting in the D-meson corresponds to eq. (91) for OGE and to the local spin-orbit terms from eqs. (63) and (65). The spin-orbit splitting appears to be overpredicted by about 25 MeV, and there are also indications that nonlocal effects may play a significant role. This situation, combined with the destructive interference between OGE and confinement, makes it very difficult to draw any definite conclusions about the spin-orbit splitting in the D-meson. For the $l = 2$ states it is found that the splittings are reversed. This also has to await experimental verification for all currently known mesons with heavy quarks.

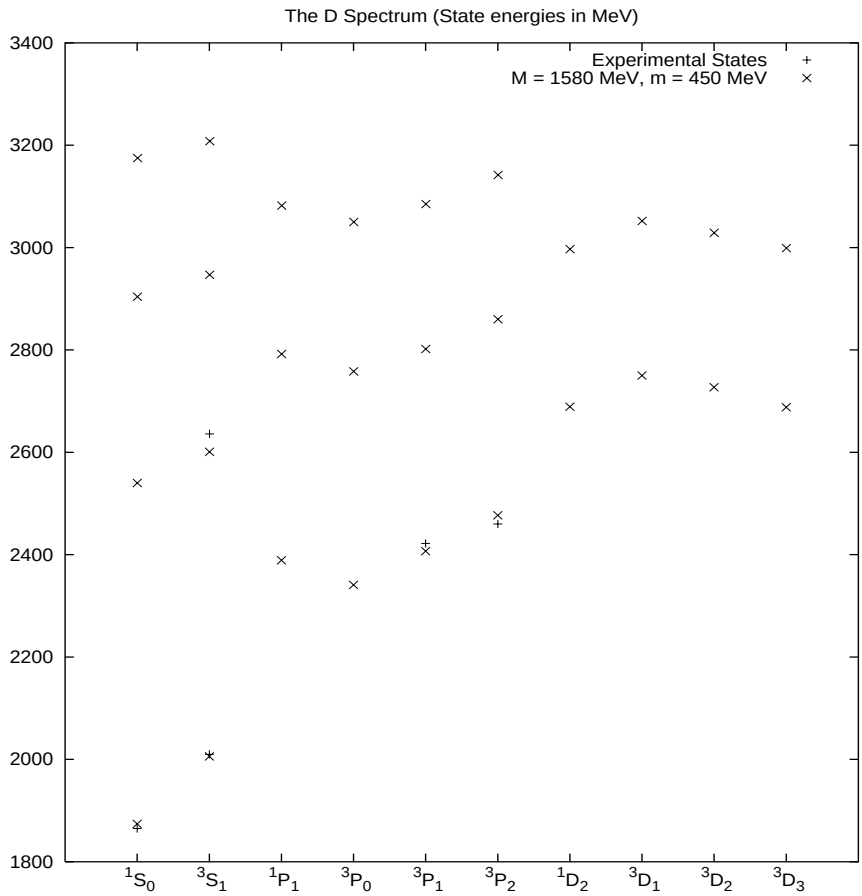

Figure 14: Calculated and experimental D meson states. These spectra display the column "$H_0 + H_{\rm HYP}$" in Table 5 as the calculated states. Experimental states are also taken from Table 5.

The calculated energies of the D_s meson states are shown in Fig. 15 and are listed in Table 6. As in the case of the D meson a satisfactory description of the still very incompletely known experimental spectrum is only achievable with a fairly large value for the constituent mass of the s quark, in this case $m_s = 560$ MeV. The overall agreement with experiment is slightly better compared to that achieved for the D meson, mainly because of the larger constituent mass of the strange quark relative to the u, d quarks. The overall structure of the D_s meson spectrum in Fig. 15 is similar to that of the D meson spectrum in Fig. 14. All four empirical states in the D_s system compare slightly better with the model predictions than is the case for the corresponding states in the D system. However, the prediction for the excited $^3S_1$ state cannot be tested since that state is yet to be observed empirically. Otherwise, the D_s spectrum is almost identical to that of the D meson.

	ϵ	H_0	$H_0 + H_{\rm HYP}$	Ref. [15]	Exp	$\sqrt{\langle r^2 \rangle}$
1^1S_0	-0.32	2075	1975	1940	1968.5±0.6	0.45
1^3S_1			2108	2130	2112.4±0.7	
2^1S_0	3.61	2706	2659	2610		0.85
2^3S_1			2722	2730		
3^1S_0	6.66	3076	3044	3090		1.20
3^3S_1			3087	3190		
4^1S_0	9.29	3356	3331			1.51
4^3S_1			3364			
1^1P_1	2.40	2539	2503	2520		0.66
1^3P_0			2455	2380		
1^3P_1			2522	2510	2535.35 ± 0.34 ± 0.5	
1^3P_2			2586	2580	2573.5 ± 1.7	
2^1P_1	5.60	2954	2928	3010		1.04
2^3P_0			2901	2900		
2^3P_1			2942	3000		
2^3P_2			2988	3060		
3^1P_1	8.31	3255	3234	3420		1.37
3^3P_0			3214	3320		
3^3P_1			3244	3410		
3^3P_2			3283	3460		
1^1D_2	4.60	2833	2817	2880		0.86
1^3D_1			2845			
1^3D_2			2844			
1^3D_3			2832			
2^1D_2	7.40	3158	3144	3290		1.22
2^3D_1			3172			
2^3D_2			3167			
2^3D_3			3157			

Table 6: Calculated and experimental D_s meson states. The first column gives the ϵ values for the spin-averaged states, and the second column gives the corresponding state energies. The third column gives the results for the complete Hamiltonian. These data are compared to ref. [15] and to experimental data when available. All energies are given in MeV. The rightmost column lists the computed rms radii of the different states in fm units.

In this context, it is worth remarking that only about 40% of the empirically determined mass difference between the D and D_s meson ground states appears to be a consequence of the difference in constituent masses of the light quarks. The rest seems to arise as a result of the nonlocal interaction components from OGE and confinement, and is reflected mostly by the parameter b in this work. However, because of the rather crude modeling of the nonlocal effects used here, more elaborate calculations are needed in order to establish the reality of this effect. Overall, the calculated D and D_s meson spectra are similar to those obtained by the Gross reduction [4] of the Bethe-Salpeter equation in ref.[15]. There, the shell spacing at increasing energy is somewhat wider, which is apparently a consequence of the inclusion of gauge-dependent retardation effects into the Hamiltonian. This effect may also reflect a difference between the Blankenbecler-Sugar and Gross quasipotential reductions, but may also be due to the employment of static potentials in ref. [15].

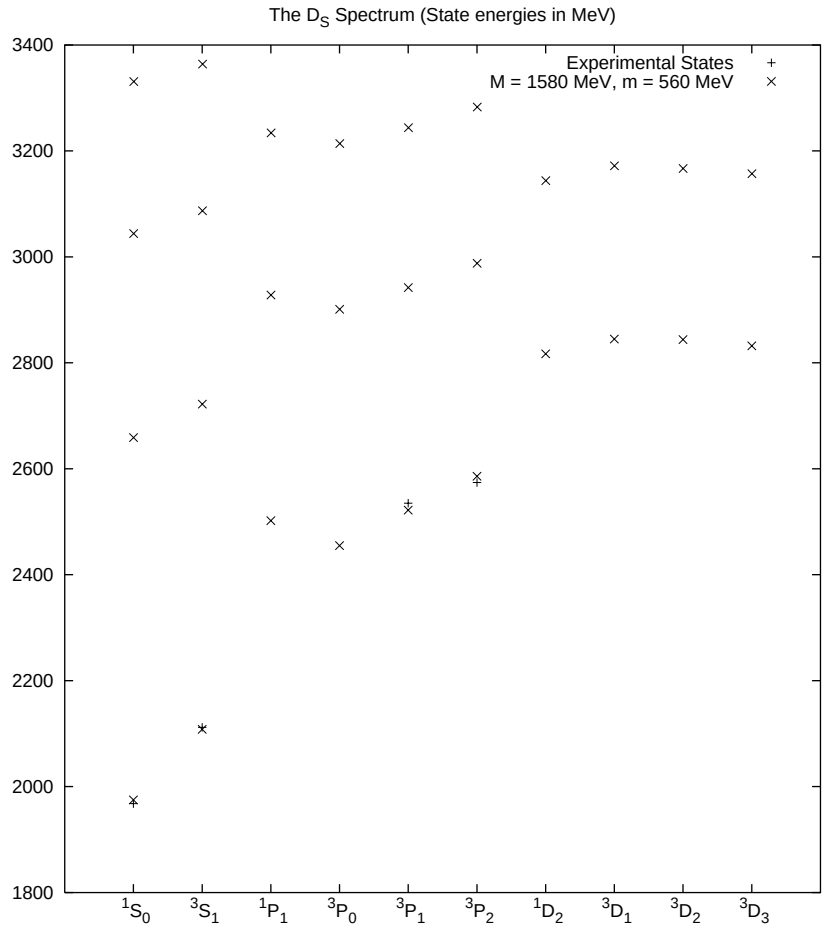

Figure 15: Calculated and experimental D_s meson states. These spectra display the column "$H_0 + H_{\rm HYP}$" in Table 6 as the calculated states. Experimental states are also taken from Table 6.

5.3 The B and B_s -meson spectra

Unfortunately, the empirical knowledge of the spectra of both the B and B_s mesons has remained very limited up to this time. For a long time only the $^1S_0$ ground states were detected experimentally. At this time, things have improved somewhat, since the ground state pseudoscalar and vector meson state energies are now known with certainty. In addition one orbital excitation of the B meson has been discovered at approximately 5700 MeV, which presumably belongs to the $P-$shell. However, the identity of this state is still very unclear and it may indeed be comprised of several narrow and broad resonances together. In this work, that state is assigned the identity $^3P_1$, mainly because that resonance is most likely to be discovered first, as it is expected to be the narrowest of the triplet P-states. In addition to these states, ref. [14] lists an experimental value for an excited S-state around 5900 MeV, but this still has to await experimental confirmation.

	ϵ	H_0	$H_0 + H_{\rm HYP}$	Ref. [15]	Exp(B^0)	Exp($B^\pm$)	$\sqrt{\langle r^2 \rangle}$
1^1S_0	0.20	5313	5277	5280	5279.2±1.8	5278.9±1.8	0.48
1^3S_1			5325	5330	5324.9±1.8		
2^1S_0	4.26	5842	5822	5830			0.91
2^3S_1			5848	5870			
3^1S_0	7.38	6132	6117	6210			1.27
3^3S_1			6136	6240			
4^1S_0	10.06	6347	6335	6520			1.59
4^3S_1			6351				
1^1P_1	2.91	5696	5686				0.71
1^3P_0			5678	5650			
1^3P_1			5699	5690	5697±9		
1^3P_2			5704	5710			
2^1P_1	6.22	6030	6022				1.10
2^3P_0			6010	6060			
2^3P_1			6028	6100			
2^3P_2			6040	6120			
3^1P_1	9.01	6266	6259				1.44
3^3P_0			6242	6390			
3^3P_1			6260				
3^3P_2			6277				
1^1D_2	5.09	5925	5920	5970			0.92
1^3D_1			6005				
1^3D_2			5955				
1^3D_3			5871				
2^1D_2	7.99	6183	6179	6310			1.28
2^3D_1			6248				
2^3D_2			6207				
2^3D_3			6140				

Table 7: Calculated and experimental B meson states. The first column gives the ϵ values for the spin-averaged states, and the second column gives the corresponding state energies. The third column gives the results for the complete Hamiltonian. These data are compared to ref. [15] and to experimental data when available. All energies are given in MeV. The rightmost column lists the computed rms radii of the different states in fm units.

The calculated B and B_s meson spectra are shown in Figs. 16 and 17. The energies of these states are also listed in Tables 7 and 8, along with the empirical values that are taken from ref.[30]. The quality of the calculated spectra, as compared to the known experimental states, is quite good. The spin-spin splitting for the ground states in both the B and B_s systems is given correctly, as is the energy of the orbital excitation of the B meson at 5700 MeV, under the assumption that it corresponds to a $j = 1$ P-shell state. The overall features of the calculated bottom meson spectra are similar to those obtained with the Gross reduction [4] of the Bethe-Salpeter equation in ref. [15], although as in the case of the charm mesons, the shell spacings at higher excitation are somewhat smaller. This effect, as noted earlier, is mostly due to the retarded interactions employed in ref. [15]. However, for all empirically observed states, the current results correspond almost exactly to those obtained in ref. [15].

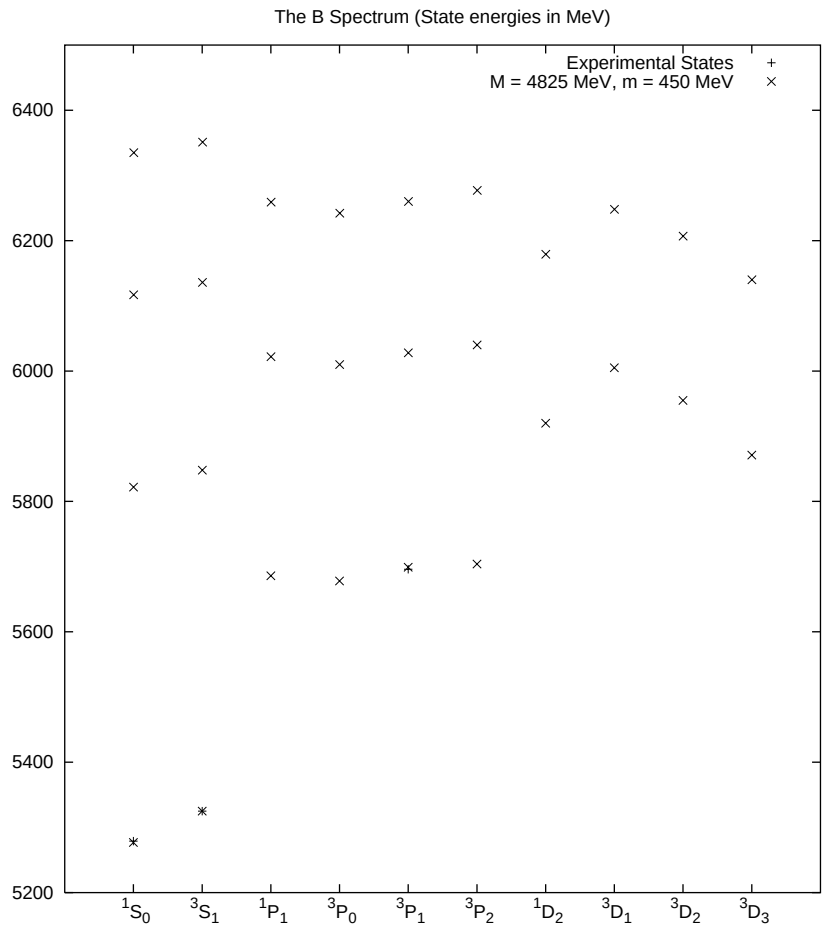

Figure 16: Calculated and experimental B meson states. These spectra display the column "$H_0 + H_{\rm HYP}$" in Table 7 as the calculated states. Experimental states are also taken from Table 7.

	ϵ	H_0	$H_0 + H_{\rm HYP}$	Ref. [15]	Exp	$\sqrt{\langle r^2 \rangle}$
1^1S_0	0.10	5404	5366	5370	5369.3±2.0	0.45
1^3S_1			5417	5430	5416.3±3.3	
2^1S_0	4.01	5959	5939	5930		0.84
2^3S_1			5966	5970		
3^1S_0	6.99	6269	6254	6310		1.18
3^3S_1			6274	6340		
4^1S_0	9.52	6500	6487	6620		1.48
4^3S_1			6504			
1^1P_1	2.73	5805	5795	5800		0.66
1^3P_0			5781	5750		
1^3P_1			5805	5790		
1^3P_2			5815	5820		
2^1P_1	5.89	6161	6153	6210		1.03
2^3P_0			6143	6170		
2^3P_1			6160	6200		
2^3P_2			6170	6220		
3^1P_1	8.53	6413	6406	6530		1.34
3^3P_0			6396	6500		
3^3P_1			6411	6520		
3^3P_2			6421	6540		
1^1D_2	4.80	6047	6043	6080		0.85
1^3D_1			6094			
1^3D_2			6067			
1^3D_3			6016			
2^1D_2	7.56	6324	6320	6420		1.20
2^3D_1			6362			
2^3D_2			6339			
2^3D_3			6298			

Table 8: Calculated and experimental B_s meson states. The first column gives the ϵ values for the spin-averaged states, and the second column gives the corresponding state energies. The third column gives the results for the complete Hamiltonian. These data are compared to ref. [15] and to experimental data when available. All energies are given in MeV. The rightmost column lists the computed rms radii of the different states in fm units.

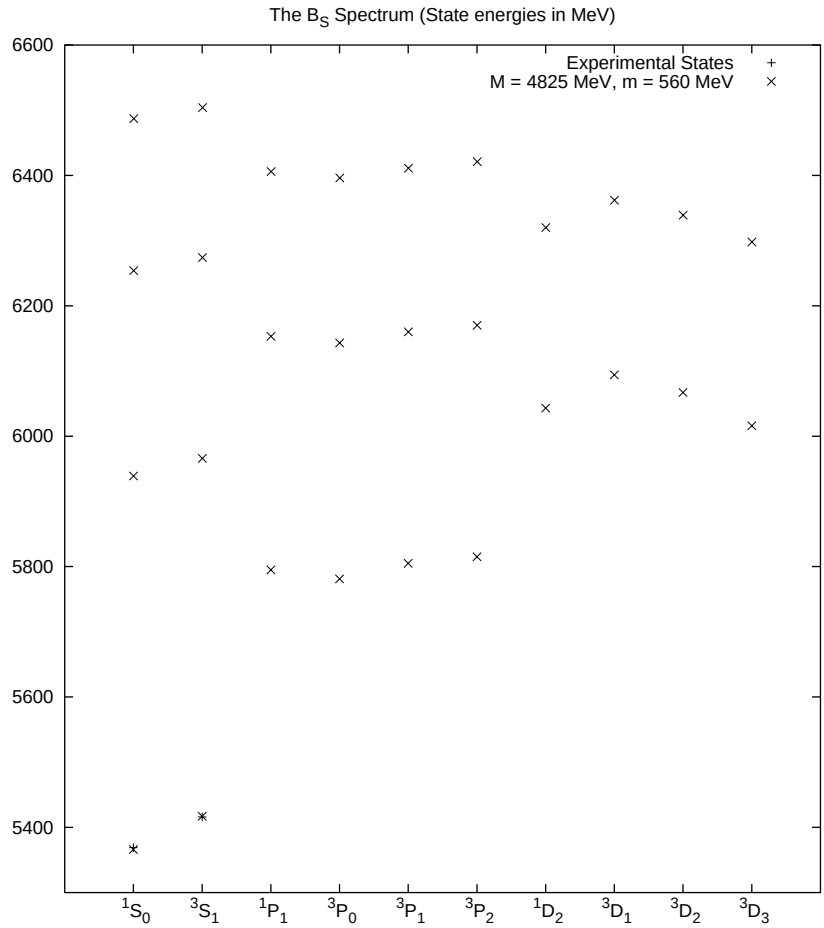

Figure 17: Calculated and experimental B_s meson states. These spectra display the column "$H_0 + H_{\rm HYP}$" in Table 8 as the calculated states. Experimental states are also taken from Table 8.

6 Discussion

Initially, the main objective was not the construction of an elaborate quark model for the calculation of heavy-light meson states, but rather the intention was merely to obtain wavefunctions suitable for computation of the M1 decay widths of heavy-light quarkonia. However, it soon became apparent that rudimentary models, while giving acceptable results for heavy quarkonia, are inadequate for the heavy-light counterparts. Several different problems arose, all of which were major obstacles since these delayed the work on the M1 transitions by several months. The most severe problems encountered can be broken up into the following distinct ones:

1. For "acceptable" values of the light constituent quark masses, the 1S-2S splittings were obtained as 300-400 MeV, while the empirically (and phenomenologically) obtained ones are typically well above 600 MeV. All attempts of compensating with the confining string constant or the parametrization of α_s were frustrated.

2. The spin-spin splittings of the ground states were only about 2/3 of what they ought to be for the charmed mesons. This effect could be eliminated by compensating with the instanton induced interaction, but this had the effect of worsening the predictions for the bottom meson spin-spin splittings, as these were about correct as given by the OGE splitting alone.

3. The most severe problem was the P-state hyperfine splitting, where the spin-orbit interaction from the confining interaction became uncontrollable as a consequence of the expansion in m^{-2}. This effect led to the $j = 2$ states being 100 MeV *below* the $j = 1$ states, although empirically they lie 40 MeV above.

4. The higher order contributions from the confining interaction constituted another serious problem. It soon became evident that especially the nonlocal contribution to the confining interaction was highly troublesome, leading to matrix elements exceeding 1 GeV in first order perturbation theory.

5. The form of α_s used was already uncomfortably strong, exceeding 1.8 at zero momentum transfer, and still the spin-spin splittings were too small.

At this stage things started to look discouraging. Naturally, doubts about the numerical algorithms began to accumulate, but since they were thoroughly tested, it was concluded that the problems were indeed of a non-trivial character. The logical way to proceed was then to analyze the abovementioned problems one by one and develop some kind of fixes for them.

A key point to note was that the 1S-2S splitting is extremely sensitive to the quark masses used, and especially to that of the light quark. This is natural, since the relativistic dampening of the kinetic energy increases rapidly with higher excitation number and lower quark masses. Thus it was concluded that raising the quark masses may have a desirable effect on the spectrum as a whole. After computations were performed, this was indeed found to be the case, but the results were quite unexpected: Agreement with experiment could be achieved only with light quark masses of 650-750 MeV ! Although not directly disastrous for a quark model concerned only with the prediction of quarkonium states, for M1 transitions, for example, the results cannot be expected to be realistic.

The problem was found to be the nonlocal contribution to the OGE interaction. Since this effect had been entered into the Hamiltonian in first order perturbation theory, the "spin-averaged" states were 100-150 MeV above the true spin-average (for S-states). By working out the expression for $f_2(r)$, eq. (88), this effect was included directly into the quarkonium wavefunctions through the RKN algorithm. This immediately had the desired consequence of giving almost correct 1S-2S splittings for all heavy-light mesons once the wavefunctions corresponded to the spin-averaged energies.

At this stage, the most severe problems had been corrected by taking into account the nonlocal effects in the OGE interaction. An unexpected benefit was that the spin-spin splitting problem corrected itself automatically, provided that the instanton induced interaction was dropped. This is not surprising in view of the crude approximations inherent in the current form of the instanton induced interaction. Consequently, the spin-spin splittings of the charmed mesons are only slightly underpredicted, while those obtained for the bottom mesons accurately reproduce the empirically observed ones.

The remaining defect in the model was that concerning the spin-orbit splittings of the P-states. This problem was dealt with by first constructing an unapproximated expression for the OGE spin-orbit interaction, which dampens it considerably, and finally by continuing the expansion of the local confining spin-orbit interaction to order m^{-4}. After these modifications, the spin-orbit splittings are only slightly overpredicted. All the empirical states are given in the correct order.

Lastly, it was found that the best way to deal with the confining interaction in the formalism used here is to approximate the nonlocal contribution by a constant, to be subtracted in the RKN algorithm. Many other papers also include a (usually negative) constant term in the confining interaction, although no previous work interprets the subtracted constant in the same way is done here. Although this approximation cannot be directly validated by rigorous mathematical arguments, it still makes it possible to obtain realistic spectra for all mesons considered. It should also be stressed that very little freedom in the choice of b was allowed in the calculations. It is also unlikely that a strong velocity dependence in the interaction remains when the full spinorial structure is employed without approximation.

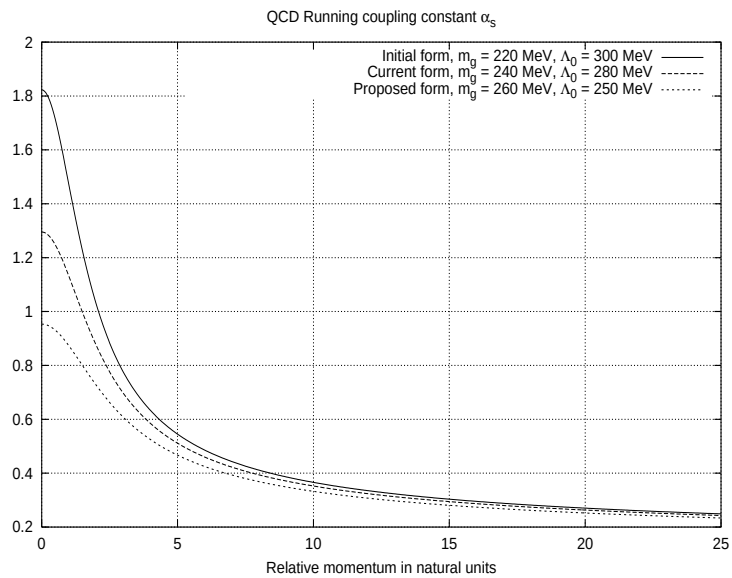

Figure 18: Different considered forms for α_s, corresponding to eq. (86). Note the close agreement at large momentum transfer.

Although the most serious problems were corrected by the abovementioned modifications, there still exists several defects in the model, which are more severe for heavy-light quarkonia than for $c\bar{c}$ or $b\bar{b}$. The most striking is the parametrization of α_s. Although the present form used in this work agrees satisfactorily with lattice calculations in the charmonium-bottomonium range, the limiting value at zero momentum transfer still exceeds 1.2. Although this is no longer disastrous, it would be highly desirable to be able to lower this to around 0.8-0.9 as indicated by recent nonperturbative analyses [23]. Another problem is that although the nonlocal effects are now at least satisfactorily

modeled, they are still expected to lead to (possibly large) underestimates of the 1S-2S splitting for an arbitrary set of quark masses, since the next term in the (asymptotic) $\vec{P}$-expansion has opposite sign. Unfortunately, very little can be done about this in the present formalism, since it is limited to expansions in $\vec{P}$ up to second order.

Recent calculations not included in this work have helped shed some light on these remaining problems. One obvious improvement which has been recently implemented is to insert the spin-spin interaction directly into the RKN algorithm rather than to treat it perturbatively. This immediately had the desirable effect of enabling a lowering of the limiting value of α_s so that it is less than 1, see Fig. 18. This was necessary in order to retain the satisfactory description of the spin-spin splittings of the S-states. However, this led to the reappearance of an earlier problem: In order to maintain the proper 1S-2S splitting of order 600 MeV for the heavy-light mesons, the light quark mass again had to be increased to around 700 MeV. If this mass is kept low, underpredictions of the excited states of about 100 MeV would occur.

The abovementioned results indicate that the only major problem left is that of truncation of the expansion to order $\vec{P}^2$. It may thus be conjectured that if the model for the quark-antiquark interaction would be solved exactly in momentum space, at least for the OGE interaction, good results could be obtained for realistic values of all parameters in the model. It would be even more rewarding to treat the linear confining interaction exactly in momentum space as well, since this would improve the consistency of the calculations. It would also be favorable to include the instanton induced interaction in some form, since this would provide a natural connection to light quark physics. This would clearly be a superior approach compared to a simple extrapolation of heavy quark physics to the light sector.

References

[1] E.J. Eichten and C. Quigg, Phys. Rev. **D52**, 1726 (1995)

[2] R. Blankenbecler and R. Sugar, Phys. Rev. **142**, 1051 (1966)

[3] A.A. Logunov and A.N. Tavkhelidze, Nuovo Cimento **29**, 380 (1963)

[4] F. Gross, Phys. Rev. **186**, 1448 (1969)

[5] M. Chemtob, J.W. Durso and D.O. Riska, Nucl. Phys. **B38**, 141 (1972)

[6] F. Coester and D.O. Riska, Ann. Phys. **234**, 141 (1994)

[7] E.H. Lomon and M.H. Partovi, Phys. Rev. **D2**, 1999 (1980)

[8] E. Hummel and J.A. Tjon, Phys. Rev. **C42**, 423 (1990)

[9] V.B. Mandelzweig and S.J. Wallace, Phys. Lett. **B197**, 469 (1987)

[10] G.S. Bali, K. Schilling and A. Wachter, Phys. Rev. **56**, 2566 (1997)

[11] D. Diakonov and V. Petrov, Physica Scripta, in press. eprint hep-lat/9810037

[12] R. Lewis and R.M. Woloshyn, eprint hep-lat/0003011

[13] C.S. Celenza, B. Huang, C.M. Shakin and H.S. Wang, Phys. Rev. **C60**, 025202 (1999)

[14] D. Ebert, R. Faustov and V.O. Galkin, Phys. Rev. **D57**, 5663 (1998), **D59**, 1019902 (1999)

[15] J. Zeng, J.W. Van Orden and W. Roberts, Phys. Rev. **D52**, 5229 (1995)

[16] S. Godfrey and N. Isgur, Phys. Rev. **D32**, 189 (1985)

[17] T.A. Lähde, C.J. Nyfält and D.O. Riska, Nucl. Phys. **A645**, 587 (1999)

[18] T.A. Lähde, C.J. Nyfält and D.O. Riska, Nucl. Phys. **A**, in press. eprint hep-ph/9908485

[19] P.G. Blunden, D.O. Riska and K. Tsushima, Nucl. Phys. **A559**, 543 (1993)

[20] M. Kirchbach, D.O. Riska and K. Tsushima, Nucl. Phys. **A542**, 616 (1992)

[21] D. Gromes, Phys. Lett. **B202**, 262 (1988)

[22] C.T.H. Davies et al., Phys. Rev. **D56**, 2755 (1997)

[23] A.C. Mattingly and P.M. Stevenson, Phys. Rev. **D49**, 437 (1994)

[24] M.-C. Chu, J.M. Grandy, S. Huang and J.W. Negele, Phys. Rev. **D49**, 6039 (1994)

[25] T. Schäfer and E.V. Shuryak, Rev. Mod. Phys **70**, 323 (1998)

[26] S. Chernyshev, M.A. Nowak and I. Zahed, Phys. Lett. **B350**, 238 (1995)

[27] S. Chernyshev, M.A. Nowak and I. Zahed, Phys. Rev. **D53**, 5176 (1996)

[28] C.J. Nyfält, M.Sc. Thesis, in preparation.

[29] J. Linde and H. Snellman, Nucl. Phys. **A619**, 346 (1997)

[30] C. Caso et al., Eur. Phys. Journal **C3**, 1 (1998)

[31] C. Bourdarios, eprint hep-ex/9811014

[32] V. Ciulli, eprint hep-ex/9911044

[33] M.A. Nowak, M. Rho and I. Zahed, *Chiral Nuclear Dynamics*, World Scientific, Singapore (1996)

[34] D. Lurié, *Particles and Fields*, Interscience publisher, Wiley & sons, Haifa 1968

[35] J.D. Bjorken and S.D. Drell, *Relativistic Quantum mechanics*, McGraw-Hill, 1964

[36] F. Halzen and A.D. Martin, *Quarks & Leptons*, John Wiley & sons, 1984

[37] M.E. Peskin and D.V. Schroeder, *An Introduction to Quantum Field Theory*, Perseus Books, Reading, Mass. 1995

[38] E. Kreyszig, *Advanced Engineering Mathematics*, 7th ed. John Wiley & sons, 1993

[39] G.B. Arfken and H.J. Weber, *Mathemathical Methods for Physicists*, Academic Press, 4th edition, 1995

[40] S. Gasiorowicz, *Quantum Physics*, 2nd ed. John Wiley & sons, 1996